Electronic Supplementary Material (ESI) for Journal of Materials Chemistry A.
This journal is © The Royal Society of Chemistry 2014

Supporting Information

Pentacenequinone derivatives for preparation of gold nanoparticles: Facile Synthesis and Catalytic Application

Kamaldeep Sharma nee Kamaldeep, Sandeep Kaur, Vandana Bhalla,* Manoj Kumar and Ankush Gupta

Department of Chemistry, UGC Centre for Advanced Studies-I, Guru Nanak Dev University, Amritsar, Punjab -143005- INDIA

vanmanan@yahoo.co.in

S3-S5 Comparison table.

S6 General experimental procedures.

S7 Synthesis of gold nanoparticles and catalysis of *p*-nitroaniline.

S8 Absorption spectra of derivative **3** showing the variation of absorption intensity in a H_2O/THF mixture with different water fractions and pictorial representation of derivative **3**.

S9 Dependence of I/I_o ratios of derivative **3** on the solvent composition of the H_2O/THF mixture and SEM images of aggregates of derivative **3** in 60%, 80% and 90% H_2O/THF mixture.

S10 SEM images of aggregates of derivatives **4** and **6** in 60% and 90% H_2O/THF mixture.

S11 UV-vis spectra of compound **3** upon additions of various metal ions as their perchlorate and chloride salt in H_2O/THF.

S12 Competitive and selectivity graph of derivative **3** to various metal ions and UV-vis spectra of compound **3** upon various additions of Au^{3+} ions in H_2O/THF.

S13 Graphical representation of rate of formation of gold nanoparticles

S14 Stern-Volmer plot of aggregates of derivative **3.**

S15 Fluorescence spectra of derivative **3** upon additions of various metal ions as their perchlorate and chloride salt in H_2O/THF.

S16 Overlay ^1H NMR spectra of **3** and gold nanoparticles of **3** after filteration with THF.

S17 Fourier transforms infrared absorption spectra for compound **3** and gold after filteration with THF.

S18 UV-vis spectra of compound **3** upon various additions of Au^{3+} ions in THF and Polarised optical microscope (POM) image of derivative **3**.

S19 XRD diffraction patterns of gold nanoparticles of derivative **3** and UV-vis spectra of 4-Bromobenzonitrile (10 μM) upon various additions of Au^{3+} ions in H_2O/THF.

S20 SEM image of gold nanoparticles of 4-Bromobenzonitrile.

S21 Absorbance and Fluorescence spectra of compound **4** showing the variation of absorbance and fluorescence intensity in H_2O/THF mixture from 0 to 90%.

S22 Absorbance and Fluorescence spectra of compound **6** showing the variation of absorbance and fluorescence intensity in H_2O/THF mixture from 0 to 90%.
S23 Absorbance and Fluorescence spectra of **4** upon addition of Au^{3+} ions in H_2O/THF (9/1**)**.
S24 Absorbance and Fluorescence spectra of **6** upon addition of Au^{3+} ions in H_2O/THF (9/1**)**.
S25 XRD diffraction patterns of gold nanoparticles of derivatives **4** and **6**.
S26 Transmission electron microscope (TEM) images and size distribution of gold nanoparticles of derivatives **3**, **4**, and **6**.
S27 Graphical representation of Time vs. absorbance plot and regression plot for the reduction of *p*-nitroaniline catalyzed by gold nanoparticles of derivatives **3**, **4** and **6**.
S28 UV-vis spectra for the reduction of *p*-nitroaniline by adding $NaBH_4$ aqueous solution using gold nanoparticles of derivatives **4** and **6** as catalysts.
S29 ^{1}H NMR of spectrum of *p*-phenylenediamine.
S30 ^{1}H NMR of spectrum of derivative **3**.
S31 Mass spectrum of compound **3**.
S32 ^{1}H NMR of spectrum of derivative **4**.
S33 ^{13}C NMR of spectrum of derivative **4**.
S34 Mass spectrum of compound **4**.
S35 ^{1}H NMR of spectrum of derivative **5**.
S36 ^{13}C NMR of spectrum of derivative **5**.
S37 Mass spectrum of compound **5**.
S38 ^{1}H NMR of spectrum of derivative **6**.
S39 ^{13}C NMR of spectrum of derivative **6**.
S40 Mass spectrum of compound **6**.
S41 Comparison table

Table S1: Comparison of present method over other reported procedure in literature for the reduction of *p*-nitroaniline to *p*-phenylenediamine by gold nanoparticles of derivative **3**.

Reaction time for the reduction of *p*-nitroaniline to *p*-phenylenediamine	Journal
5min.	Present manuscript
30 min.	Chem. Sci., 2013, **4**, 3667.
59 min.	Ind. Eng. Chem. Res., 2013, **52**, 556.
25 min.	CrystEngComm, 2012, **14**, 7600
70 min.	J. Phys. Chem. C, 2012, **116**, 23757
17 min.	Langmuir, 2011, **27**, 3906
56 min.	J. Phys. Chem. C, 2009, **113**, 17730
20 min.	J. Phys. Chem. C, 2009, **113**, 5157
86 min.	J. Phys. Chem. C, 2009, **113**, 5150

Table S2: Comparison of present method for the preparation of gold nanoparticles over other reported procedure in literature.

Method of formation of gold nanoparticles	Size of gold nanoparticles	Reaction time to prepare gold nanoparticles	Reducing agent or surfactants	Reaction temp. (in ^{o}C)	Journals
Wet chemical method	5-10 nm	2 min.	No	Room temp.	Present manuscript
Ultrasound assisted interfacial method	143.9 ± 17.5-249.1 ± 31.3 nm	120 sec.	2-ethoxyaniline (EOA)	45	Chem. Commun., 2013, **49**, 987
Chemical method	12 nm	10 min.	$NaBH_4$	0	J. Mater. Chem.C,2013, **1**, 902.
Chemical method	20 nm	2 min	Glycerol	Room temp.	Advances in Nanoparticles, 2013, **2**, 78
Chemical method	6-17.5 nm	-	$NaBH_4$	-	Chem. Commun., 2013, **49**, 3218
Seed-mediated growth method	63.6 nm	60 min	$NaBH_4$	30	J. Phys. Chem. C 2012, **116**, 23757
Chemical method	20-50 nm	90 min	Sodium citrate	80-85	Nanoscale Research Letters 2012, **7**, 420
Seed-mediated method	56.4 ± 1.4 nm	2 h	$NaBH_4$	Ice cold solution	Phys. Chem. Chem. Phys., 2012, **14**, 9343
Chemical method	50-200 nm	15 min.	Citrate	~100	Langmuir, 2010, **26**, 3585
Chemical method	~20 nm	30 min	Tripotassium citrate	~100	J. Phys. Chem. B 2006, **110**, 17813
Wet Chemical method	Large size (Hundred nanometers)	Several hours	No	Room temp.	Chem. Commun. 2004, 1182
Wet chemical method	Micrometer sized	Several minutes	No	Room temp	Angew. Chem. Int. Ed. 2004, **43**, 6360
Wet Chemical method	4-33 nm	30-150 min.	-	80	Macromol. Rapid Commun. 2003, **24**, 1024
Wet Chemical method	5-20 nm	-	No	Room temp	Chem. Mater. 1999, **11**, 3268

Table S3: Comparison of detection limit reported in the present manuscript for detection of gold ions with other reported detection limits in the literature.

Paper Journal	System	Detection Limit
Present Manuscript	Fluorescent Aggregates H_2O/THF (6/4 v/v)	100 nM
Analyst, 2013, 138, 3638	Non aggregated form CH_3CN–HEPES buffer (1/1 v/v)	0.6 ppm
Org. Lett. 2012, 14, 5062	Non aggregated form (0.25% DMSO in HEPES)	0.4 μM
Chem. Commun. 2012, 48, 744	Non aggregated form EtOH/ PBS buffer (1/1 v/v)	320 nM
Chem. Commun. 2011, 47, 4703	Non aggregated form (0.3% DMF in PBS HEPES)	290 nM
Org. Lett. 2010, 12, 932	Non aggregated form (Ethanol)	64 ppb
Org. Lett. 2010, 12, 401	Non aggregated form CH_3CN/PBS buffer (1/1 v/v)	0.4 ppm
Chem. Commun. 2009, 7218	Non aggregated form EtOH–HEPES and DMSO–HEPES buffer (1/1 v/v)	100 ppb

General experimental Procedures:

All reagents were purchased from Aldrich and were used without further purification. THF was dried over sodium and benzophenone and kept over molecular sieves overnight before use. UV-vis spectra were recorded on a SHIMADZU UV-2450 spectrophotometer, with a quartz cuvette (path length, 1 cm). The cell holder was thermostatted at 25^0 C. The fluorescence spectra were recorded with a SHIMADZU 5301 PC spectrofluorimeter. Scanning electron microscope (SEM) images were obtained with a field-emission scanning electron microscope (SEM CARL ZEISS SUPRA 55). Polarized optical microscope (POM) images were recorded on NIKON ECLIPSE LV100 POL. Elemental analysis (C, H, N) was performed on a Flash EA 1112 CHNS-O analyzer (Thermo Electron Corp.). ^1H was recorded on a JEOL-FT NMR–AL 300 MHz spectrophotometer using $CDCl_3$ as solvent and tetramethylsilane $SiMe_4$ as internal standards. UV-vis studies were performed in THF and H_2O/THF mixture. Data are reported as follows: chemical shifts in ppm (δ), multiplicity (s = singlet, d = doublet, br = broad singlet m = multiplet), coupling constants *J* (Hz), integration, and interpretation. Silica gel (60–120 mesh) was used for column chromatography.

Synthesis of Gold Nanoparticles. To a 3 ml solution of compound **3**, **4**, and **6** (0.2 mM) was added 0.1 M $AuCl_3$ (15 µL for **3**, 45 µL for **4**, 30 µL for **6**) in H_2O/THF (6:4, v/v). The reaction was stirred at room temperature for 2 min and formations of nanoparticles take place. These nanoparticles solution was used as such in the catalytic experiment.

Catalysis of *p*-nitroaniline. 300 µL of 1 mM *p*-nitroaniline, 300 µL of 10 mM $NaBH_4$ and 5 µL (2.5 nmol) of gold nanoparticles of derivative **3**, **4**, and **6** were mixed. After that, different volumes of deionized water were added to the reaction mixture to nullify the dilution effect. After stirring the reaction mixture, a colour change of the reaction mixture from yellow to colourless was observed which indicate the reduction of *p*-nitroaniline to *p*-phenylenediamine. The reduction of *p*-nitroaniline takes 5 min. in case of derivative **3**, 24 min. in case of **4** and 18 min. in case of derivative **6**. The formation of the reduced product *p*-phenylenediamine was confirmed from the ^{1}H-NMR spectra (in $CDCl_3$) of the product (see pS29). The reduction of *p*-nitroaniline was also carried out in excess. After the complete reduction, the product was purified by column chromatography and found to be in 98% yield. ^{1}H NMR (400 MHz, $CDCl_3$): δ = 3.29 [s, 4H, NH_2], 6.57 (s, 4H, ArH].

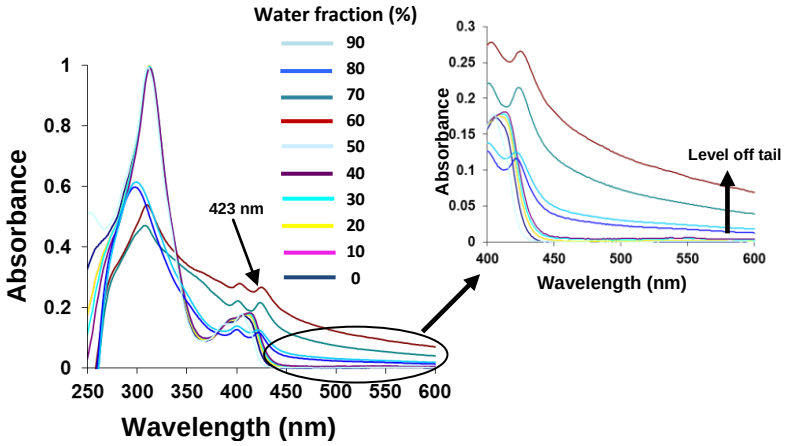

Fig. S1 Absorption spectra of derivative **3** (10 μM) showing the variation of absorption intensity in H_2O/THF mixture with different fractions of H_2O. Inset: enlarge UV-vis spectra of derivative **3** (10 μM) with the addition of H_2O/THF mixture in the range of 400-600 nm showing level-off long wavelength tail.

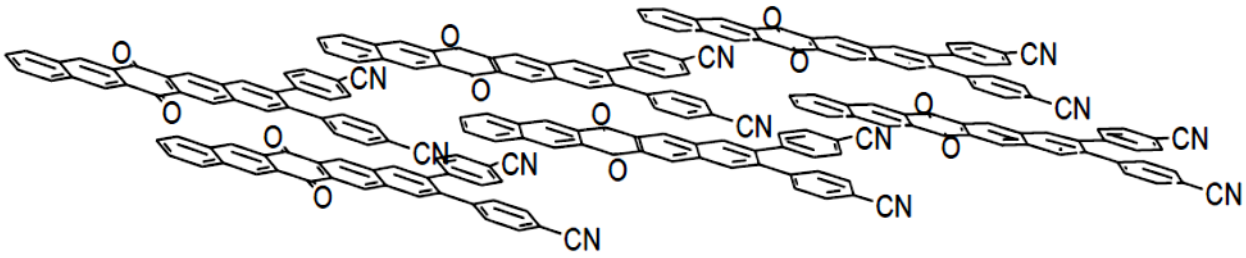

Fig. S2 Schematic view of intermolecular charge transfer (ICT) state of derivative **3** with their head to tail alignment.

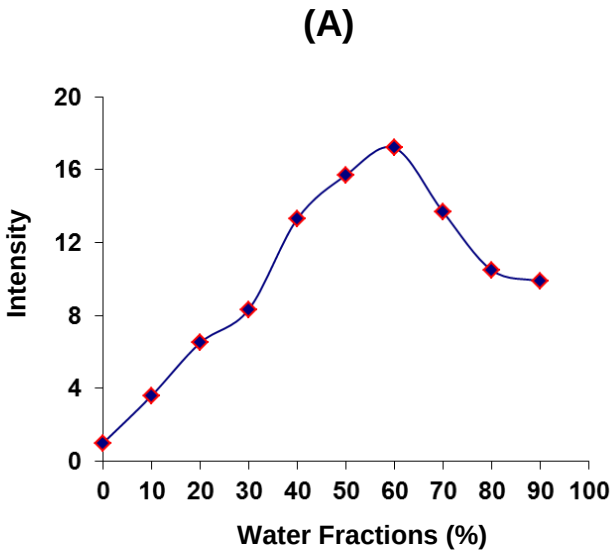

Fig. S3A Dependence of I/I_o ratios of derivative **3** on the solvent composition of the H_2O/THF mixture.

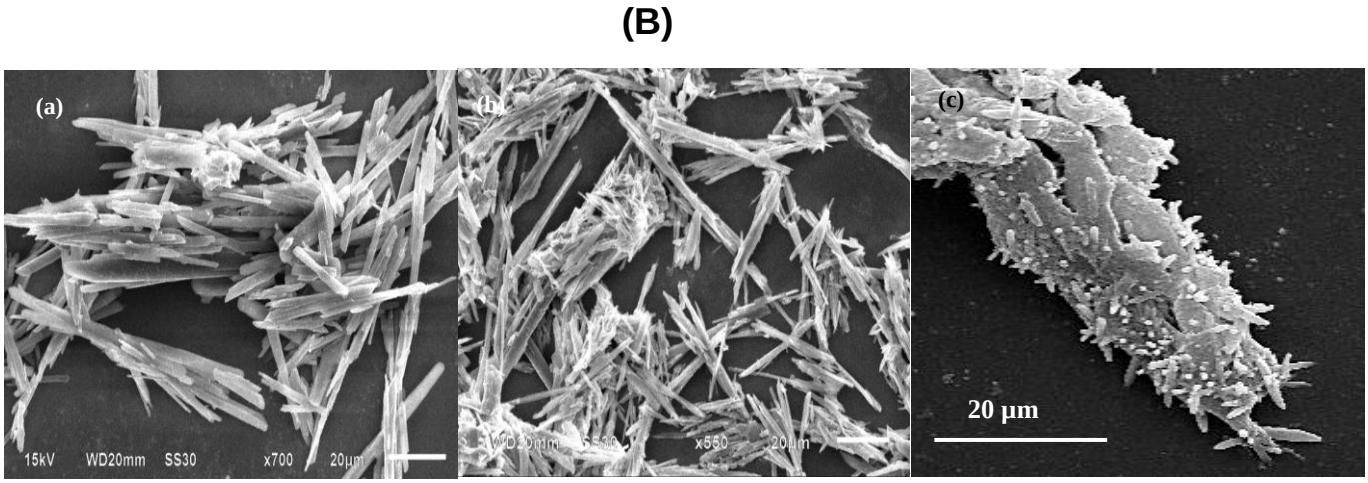

Fig. S3B SEM images of aggregates of derivative **3** in (a) 60% H_2O/THF mixture (b) 80% H_2O/THF mixture (c) 90% H_2O/THF mixture. Scale bar (a), (b) and (c) 20 µm.

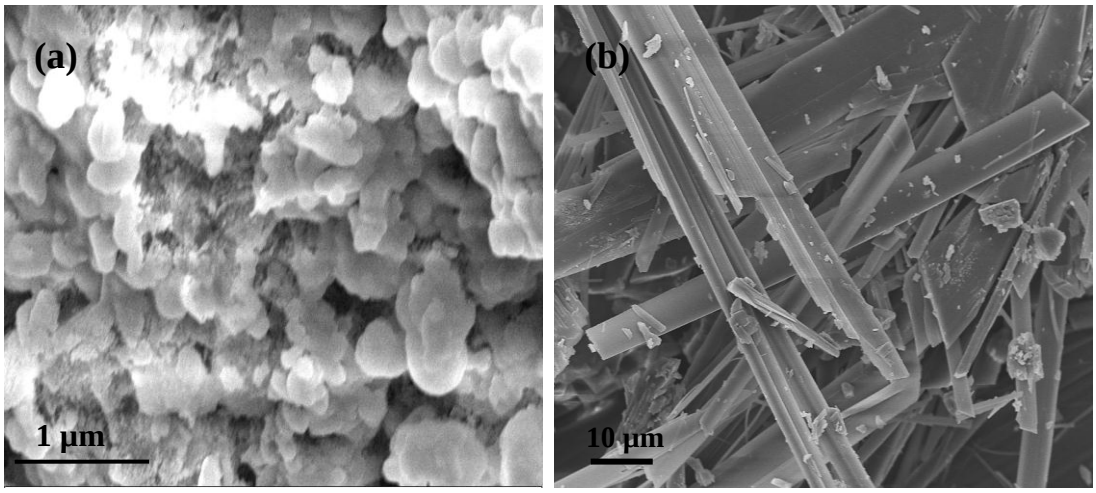

Fig. S4A SEM images of aggregates of derivative **4** (a) in 60% H_2O/THF mixture (b) in 90% H_2O/THF mixture. Scale bar (a) 1µm (b) 10 µm.

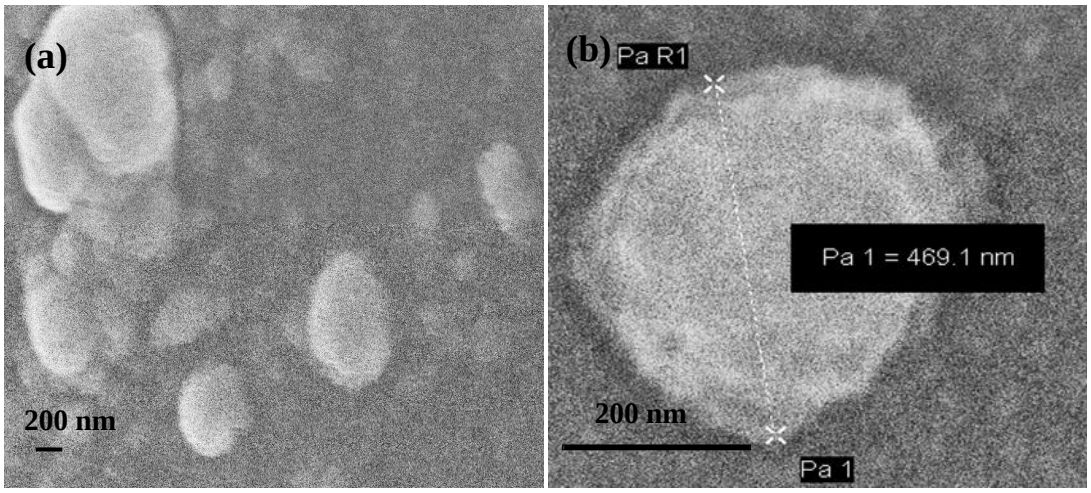

Fig. S4B SEM images of aggregates of derivative **6** (a) in 60% H_2O/THF mixture (b) in 90% H_2O/THF mixture. Scale bar (a) and (b) 200 nm.

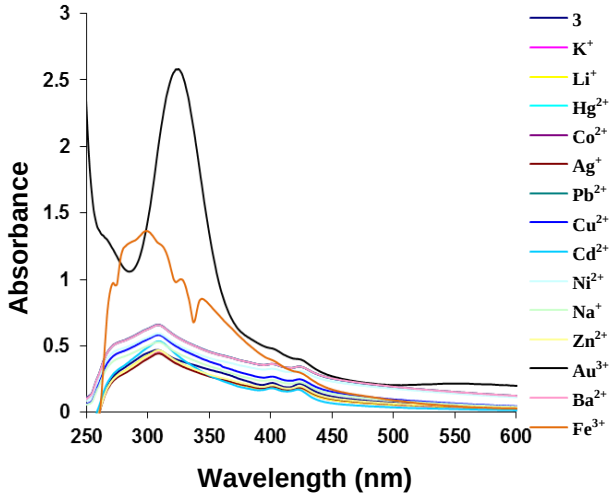

Fig. S5 UV-vis spectra of derivative **3** (10 μM) upon additions of 500 μM of various metal ions as their perchlorate salt in H_2O/THF (6/4), buffered with HEPES, pH = 7.0.

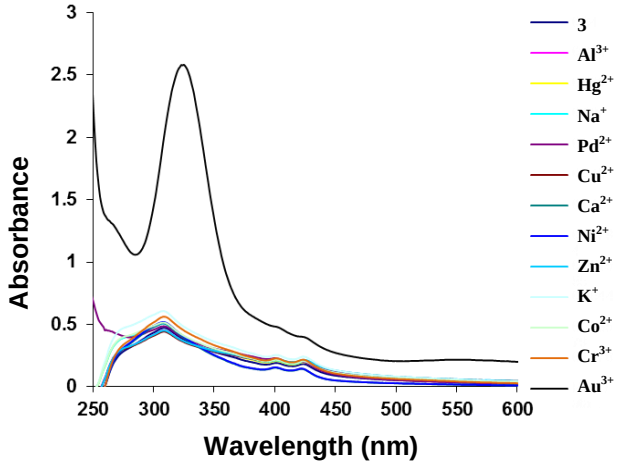

Fig. S6 UV-vis spectra of derivative **3** (10 μM) upon additions of 500 μM of various metal ions as their chloride salt in H_2O/THF (6/4), buffered with HEPES, pH = 7.0.

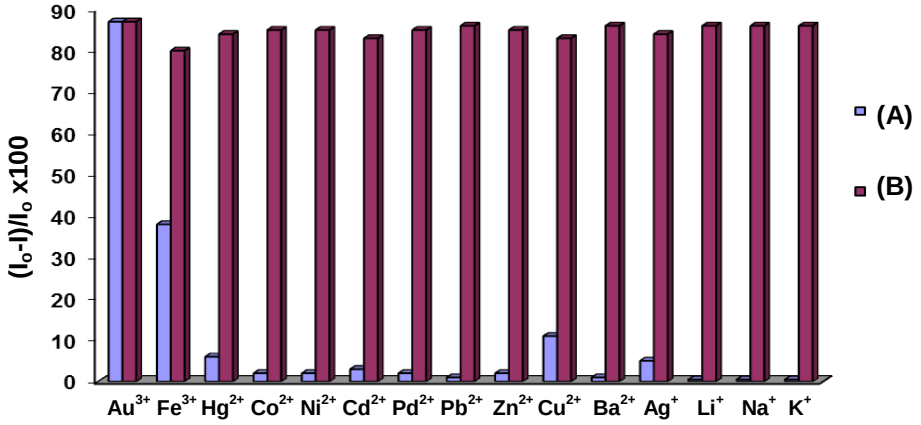

Fig. S7 Fluorescence response of derivative **3** (10 μM) to various cations (500 μM) in H_2O/THF (6/4); buffered with HEPES, pH = 7.0; λ_{ex} = 310 nm. Bars represent the emission intensity ratio $(I_o - I)/I_o \times 100$ (I_o = initial fluorescence intensity at 476 nm; I = final fluorescence intensity at 476 nm after the addition of Au^{3+} ions). (A) The sky blue bars represent the addition of individual metal ions, (B) the brown bars represent the change in the emission that occurs upon the subsequent addition of Au^{3+} (500 μM) to the above solution.

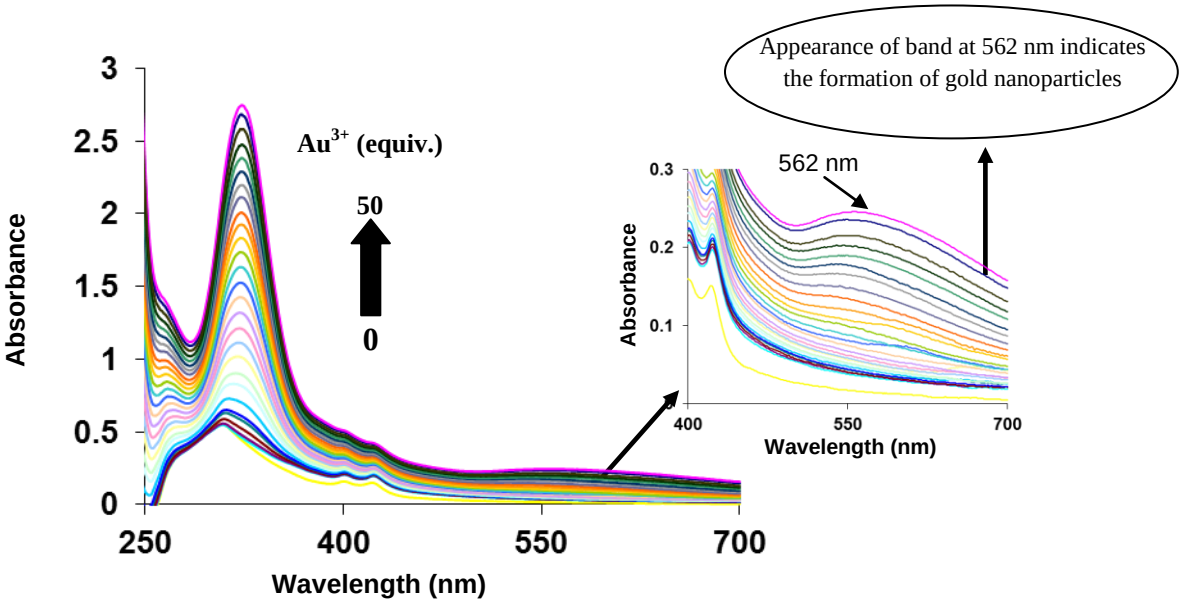

Fig. S8 UV-vis spectra of derivative **3** (10 μM) upon various additions of Au^{3+} ions in H_2O/THF (6/4). Inset: enlarge UV spectra of compound **3** (10 μM) in the range of 400-700 nm.

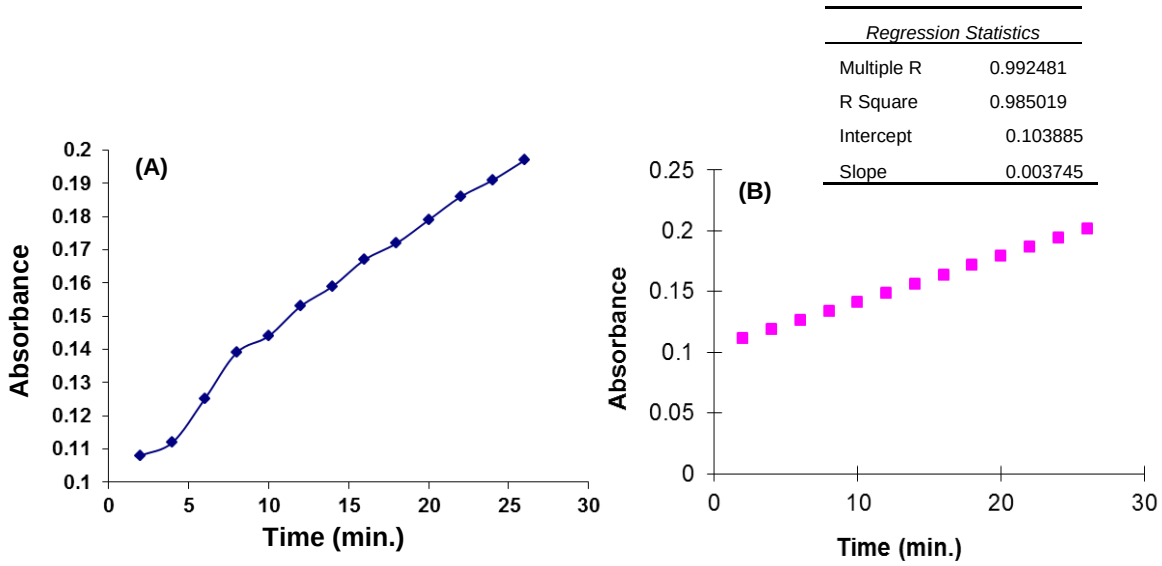

Fig. S9 Graphical representation of the rate of formation of gold nanoparticles of derivative **3**. (A) Time (min.) vs. absorbance plot at 562 nm (B) regression plot of A.

The first order[1] rate constant for the formation of gold nanoparticles was calculated from the changes of intensity of absorbance of aggregates of derivative **3** in the presence of Au^{3+} ions at different time interval[2].

From the time vs. absorbance plot at fixed wavelength 562 nm by using first order rate equation we get the rate constant = k = slope×2.303 = 1.43×10^{-3} Sec^{-1}.

[1] Luty-Błocho, M.; Pacławski, K.; Wojnicki, M.; Fitzner, K. *Inorganica Chimica Acta* **2013**, 395 189‑196.

[2] Goswami, S.; Das, S.; Aich, K.; Sarkar, D.; Mondal, T. K.; Quah, C. K.; Fun, H-K. *Dalton Trans*. **2013**, *42*, 15113–15119.

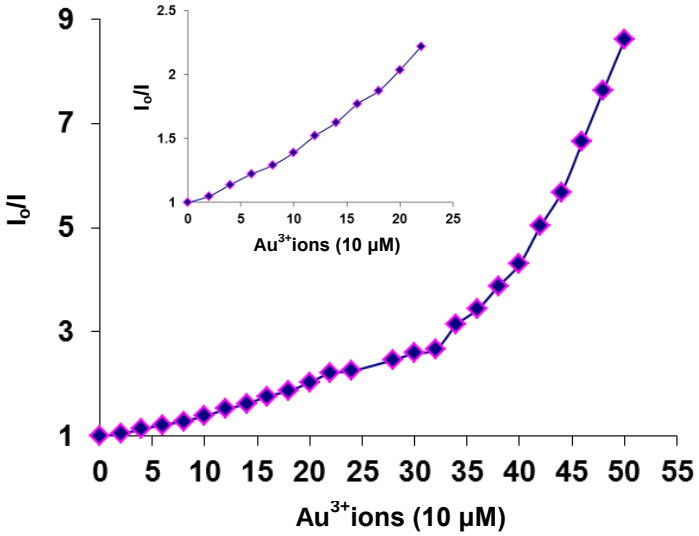

Fig. S10 Variation of fluorescence intensity of aggregates of derivative **3** (10 μM) at 476 nm in H_2O/THF (6:4, v/v) buffered with HEPES, pH =7.0, $\lambda_{ex.}$ = 310 nm in the presence of different concentrations of Au^{3+} ions (I_o/I; I_o = initial fluorescence intensity at 476 nm; I= fluorescence intensity after the addition of Au^{3+} ions at 476 nm). Inset shows the linear Stern-Volmer plot at lower concentration of Au^{3+} ions.

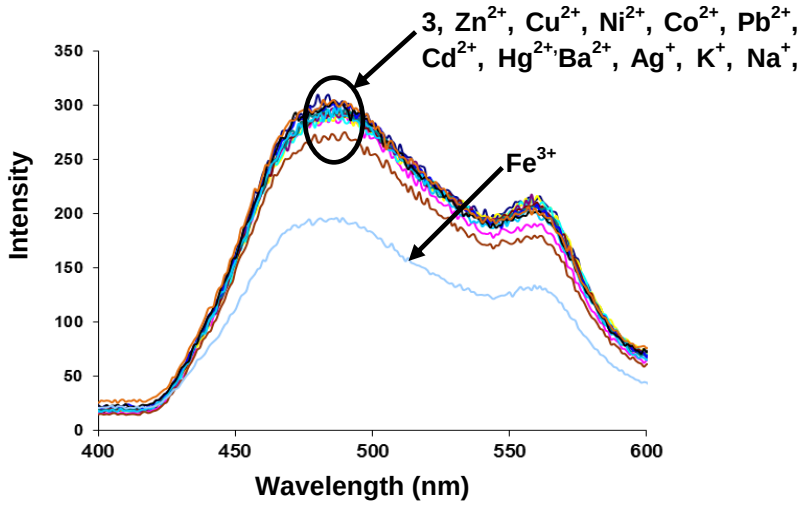

Fig. S11 Fluorescence spectra of derivative **3** (10 μM) upon additions of various metal ions (500 μM) as their perchlorate salt in H_2O/THF (6/4) buffered with HEPES, pH = 7.0.

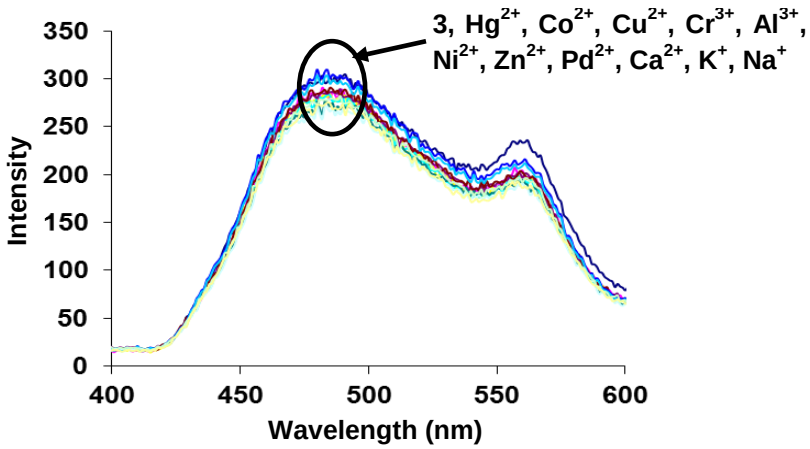

Fig. S12 Fluorescence spectra of derivative **3** (10 μM) upon additions of various metal ions (500 μM) as their chloride salt in H_2O/THF (6/4) buffered with HEPES, pH = 7.0.

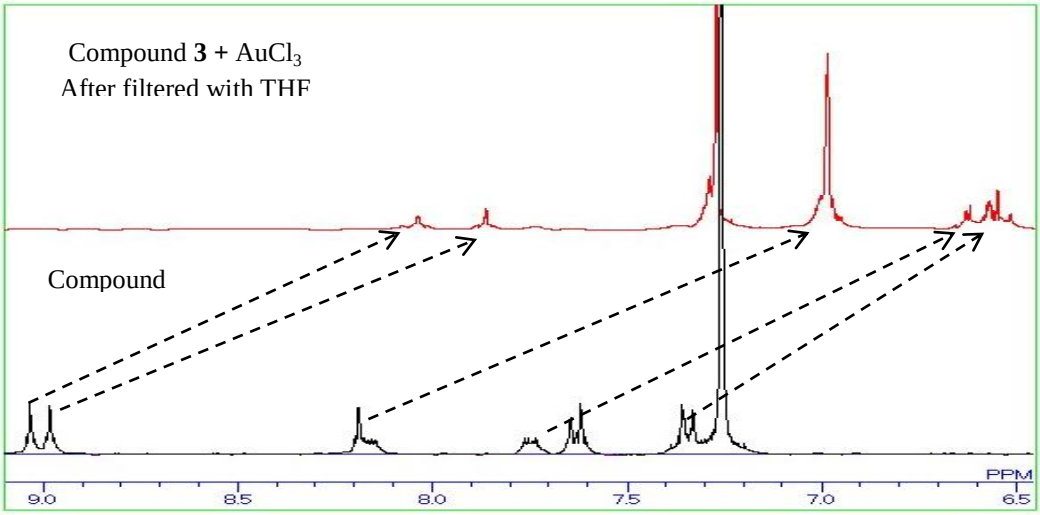

Fig. S13: Overlay ^{1}H NMR spectra of derivative **3** and gold nanoparticles of derivative **3** after filteration with THF.

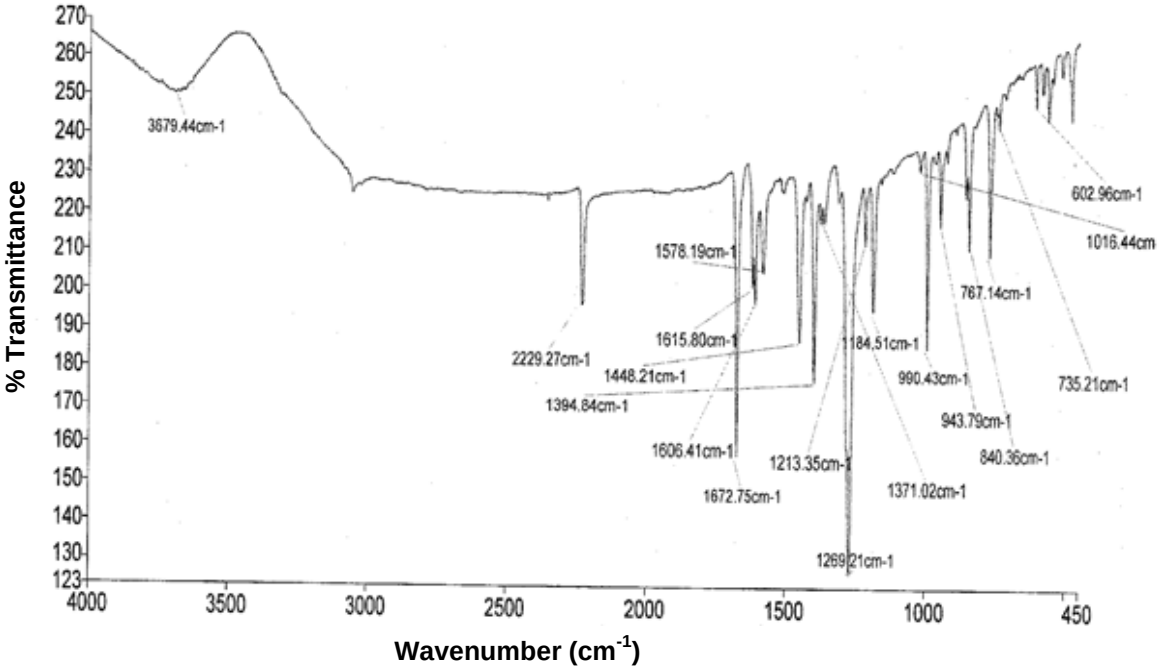

Fig. S14 Fourier transforms infrared absorption spectra of derivative **3.**

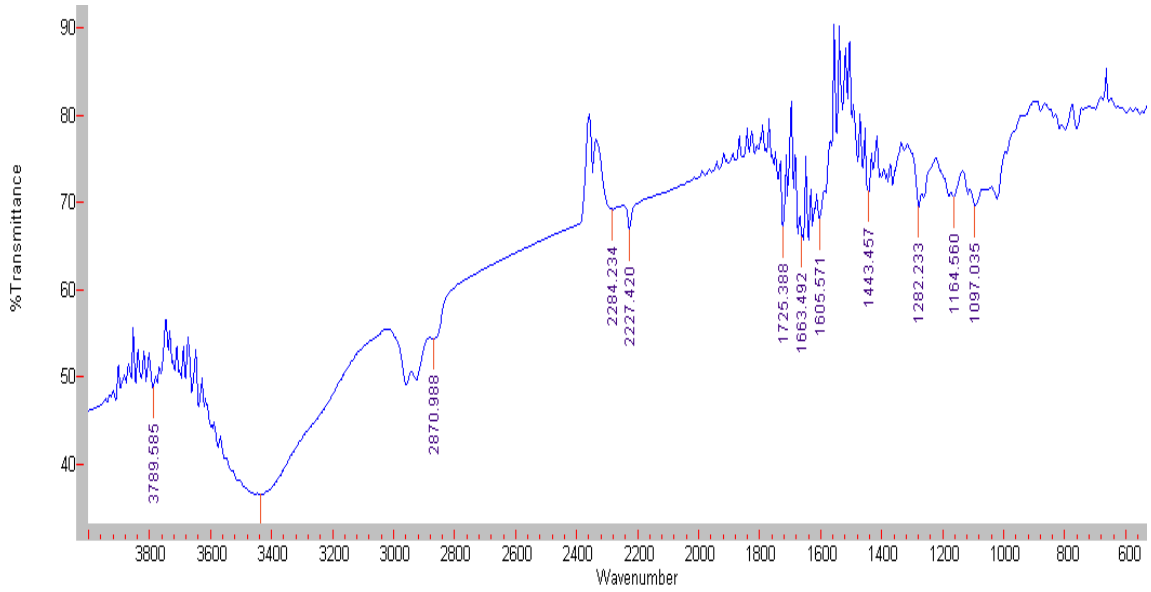

Fig. S15 Fourier transforms infrared absorption spectra of gold nanoparticles of derivative **3** after filteration with THF.

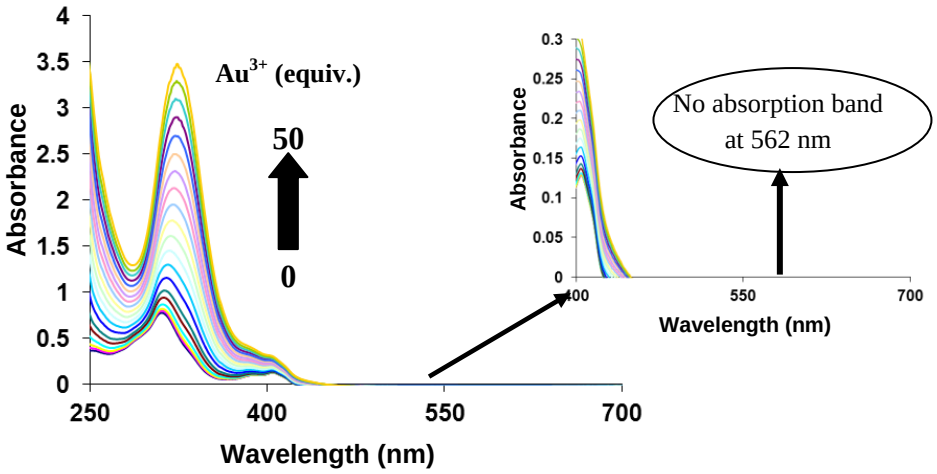

Fig. S16 UV-vis spectra of derivative **3** (10 μM) upon various additions of Au^{3+} ions in THF. Inset: enlarge UV spectra of compound **3** (10 μM) in the range of 400-700 nm.

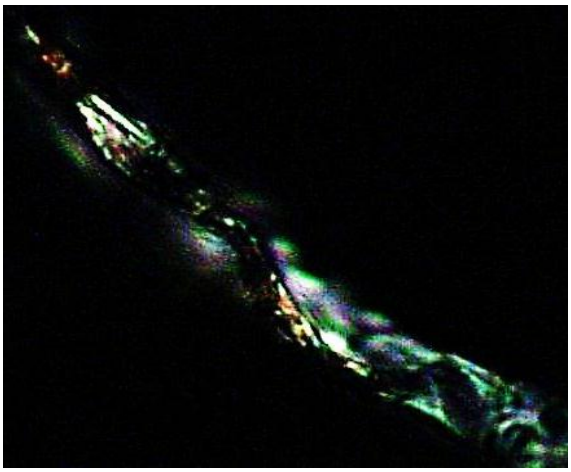

Fig. S17 Polarized optical micrograph of gold nanoparticles of derivative **3** at room temperature through crossed polarizing filters.

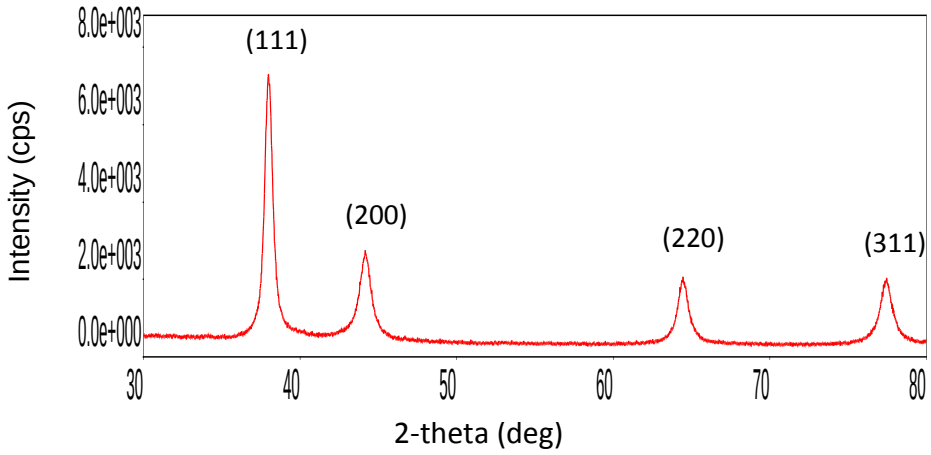

Fig. S18 Representative XRD diffraction patterns of gold nanoparticles of derivative **3**.

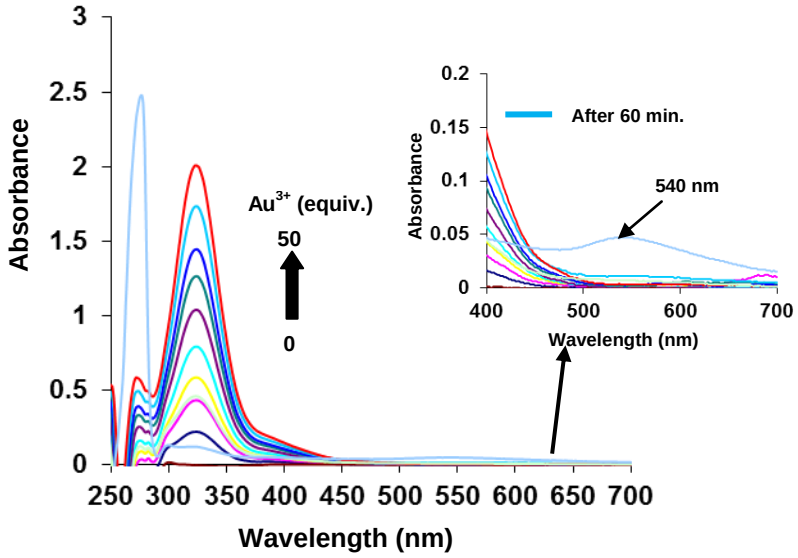

Fig. S19 UV-vis spectra of 4-Bromobenzonitrile (10 μM) upon various additions of Au^{3+} ions in H_2O/THF (6/4). Inset: enlarge UV spectra of 4-Bromobenzonitrile (10 μM) in the range of 400-700 nm.

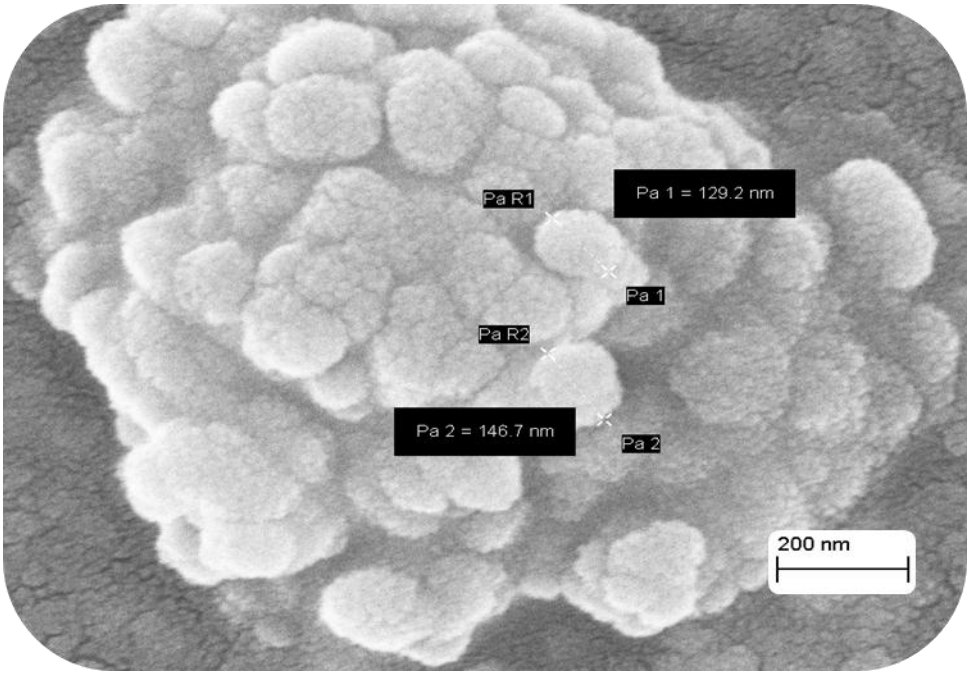

Fig. S20 SEM image of gold nanoparticles of 4-Bromobenzonitrile showing size of gold nanoparticles. Scale bar 200 nm.

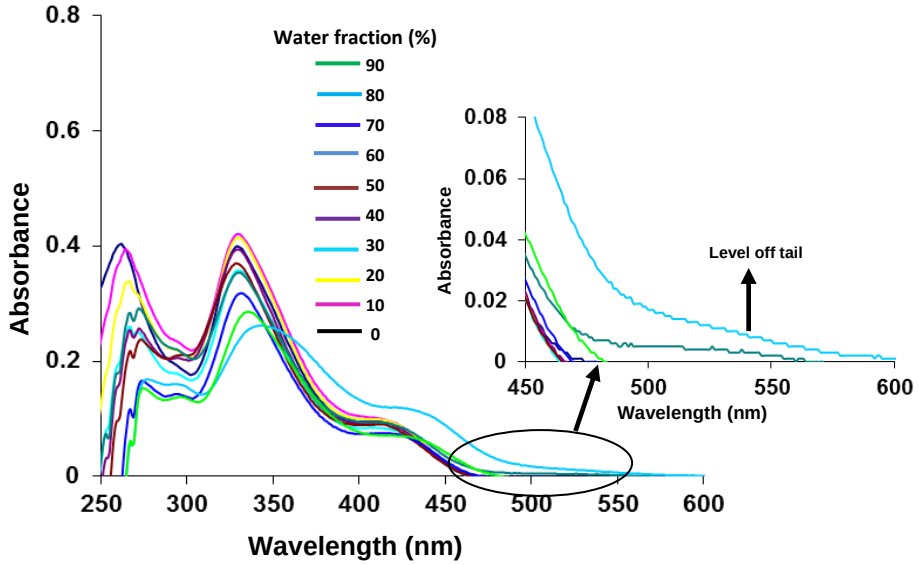

Fig. S21 Absorption spectrum of derivative **4** (10 μM) showing the variation of absorption intensity in H_2O/THF mixture with different fractions of water. Inset: enlarge UV-vis spectra of derivative **4** (10 μM) with the addition of H_2O/THF mixture in the range of 450-600 nm showing level-off long wavelength tail.

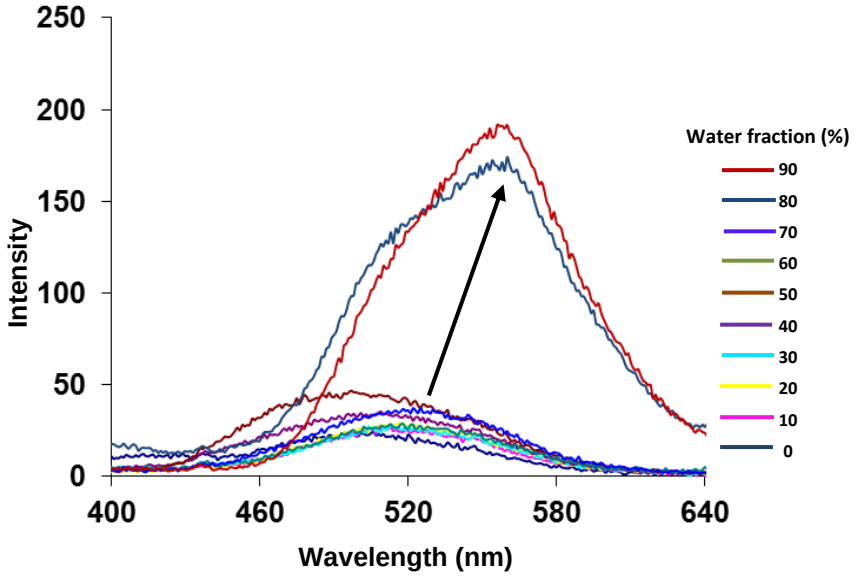

Fig. S22 Fluorescence spectrum of derivative **4** (10 μM) showing the variation of fluorescence intensity in H_2O/THF mixture from 0 to 90% volume fractions of water in THF. λ_{ex} = 327 nm.

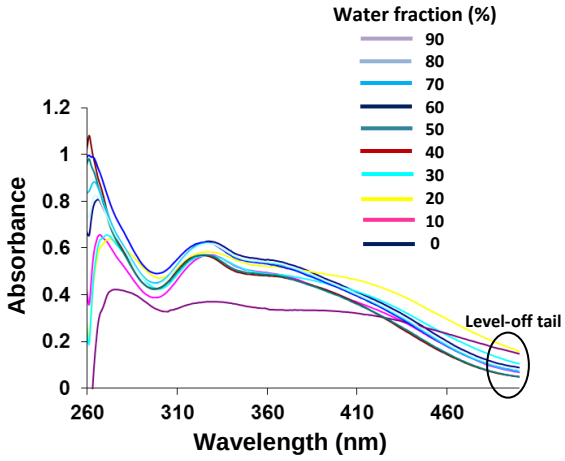

Fig. S23 Absorption spectrum of derivative **6** (10 μM) showing the variation of absorption intensity in H_2O/THF mixture with different fractions of water.

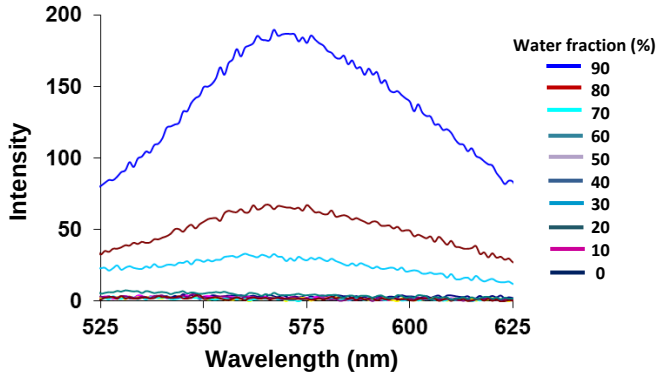

Fig. S24 Fluorescence spectrum of derivative **6** ($1x10^{-4}$ M) showing the variation of fluorescence intensity in various H_2O/THF mixtures. λ_{ex} = 322 nm.

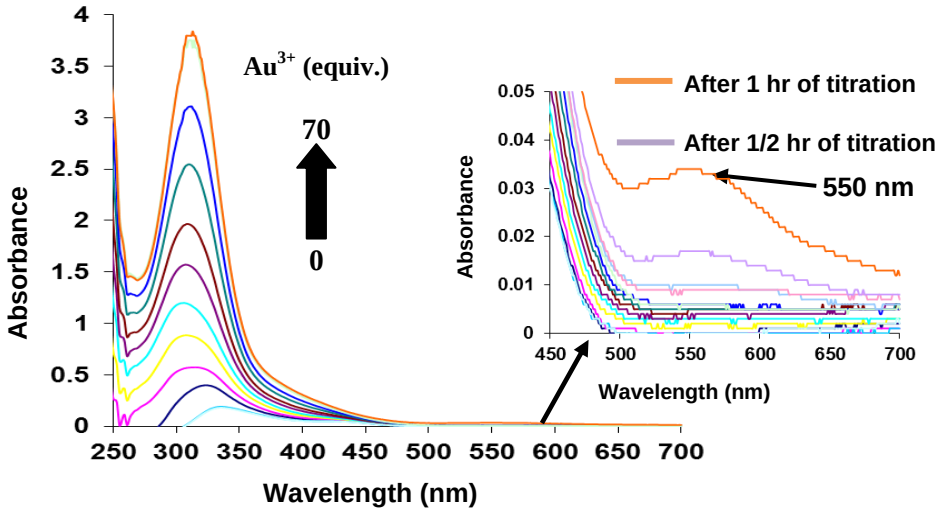

Fig. S25 UV-vis spectrum of derivative **4** (10 μM) upon various additions of Au^{3+} ions in H_2O/THF (9/1). Inset: enlarge UV spectrum of compound **4** (10 μM) in the range of 450-700 nm showing a new absorption band at 550 nm.

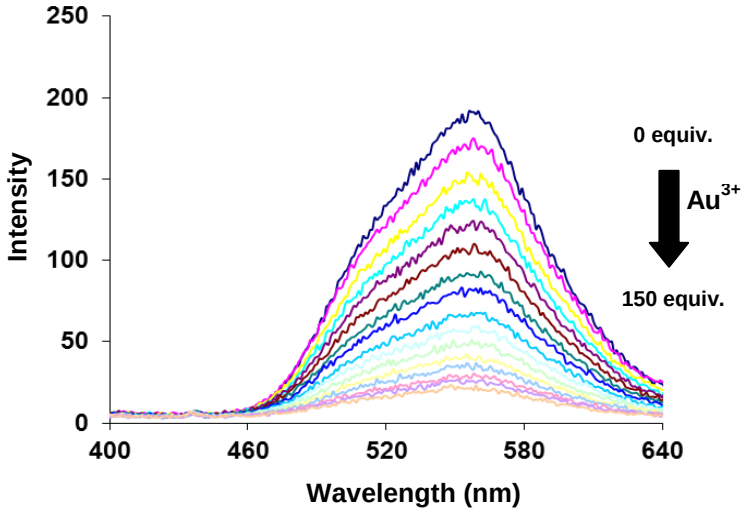

Fig. S26 Fluorescence spectrum of derivative **4** (10 μM) upon addition of Au^{3+} ions in H_2O/THF (9/1); buffered with HEPES, pH = 7.0

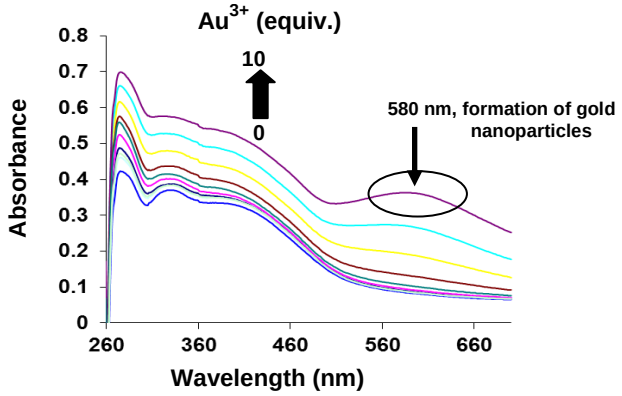

Fig. S27. UV-vis spectrum of derivative **6** (10 µM) upon addition of Au^{3+} ions (10 equiv.) in H_2O/THF (9:1) mixture; buffered with HEPES, pH = 7.0.

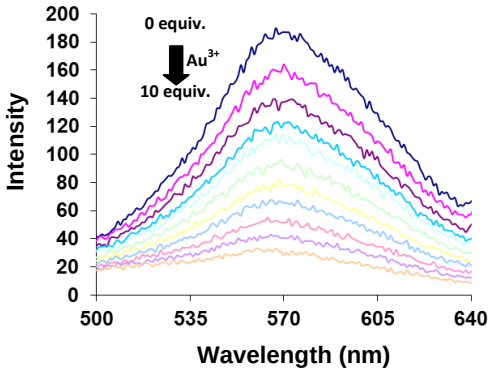

Fig. S28 Fluorescence spectrum of derivative **6** (1 x 10^{-4} µM) upon addition of Au^{3+} ions in H_2O/THF (9:1); buffered with HEPES, pH = 7.0. λ_{ex} = 322 nm

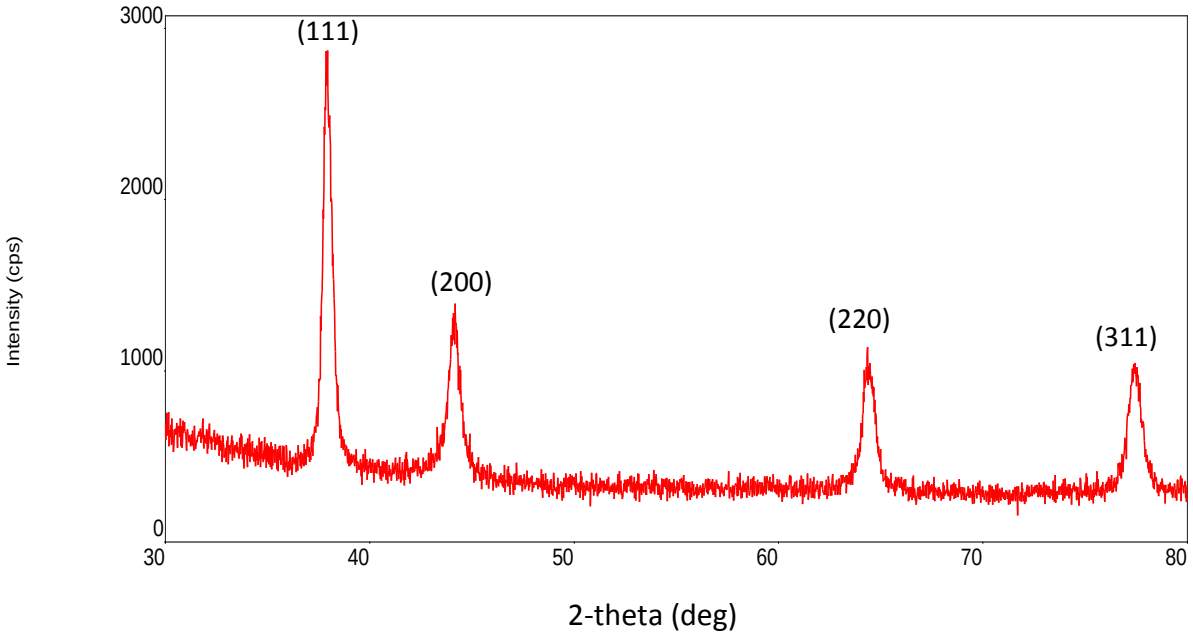

Fig. S29 Representative XRD diffraction patterns of gold nanoparticles of derivative **4**.

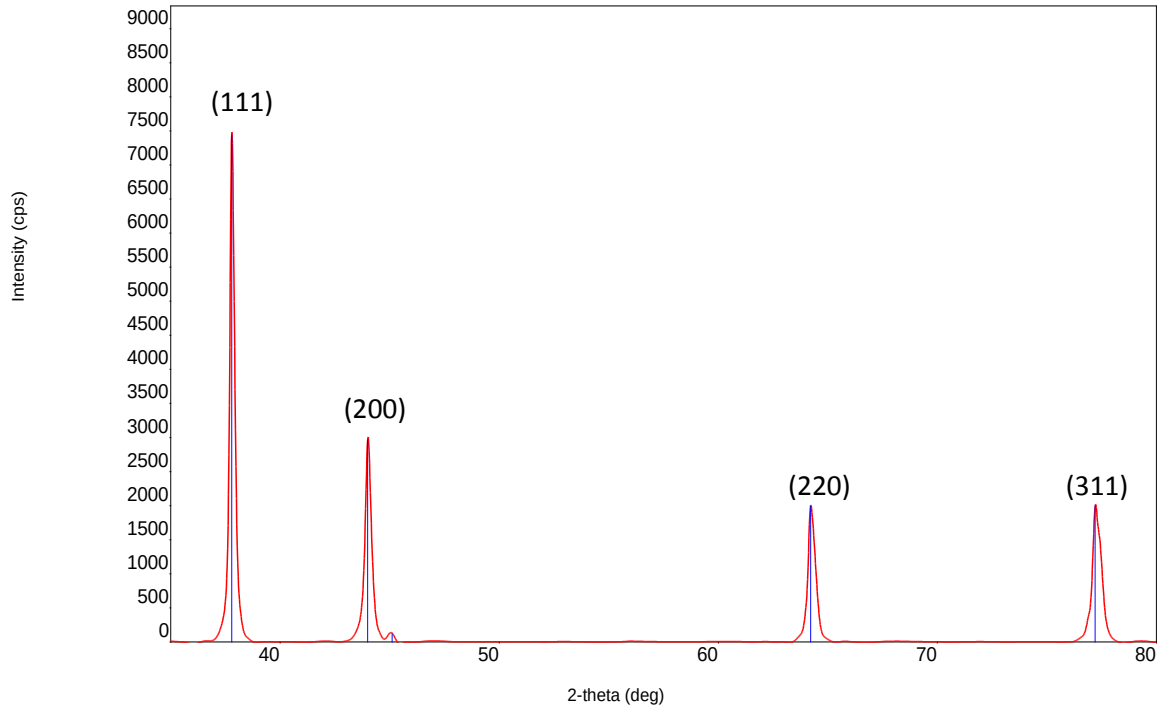

Fig. S30 Representative XRD diffraction patterns of gold nanoparticles of derivative **6**.

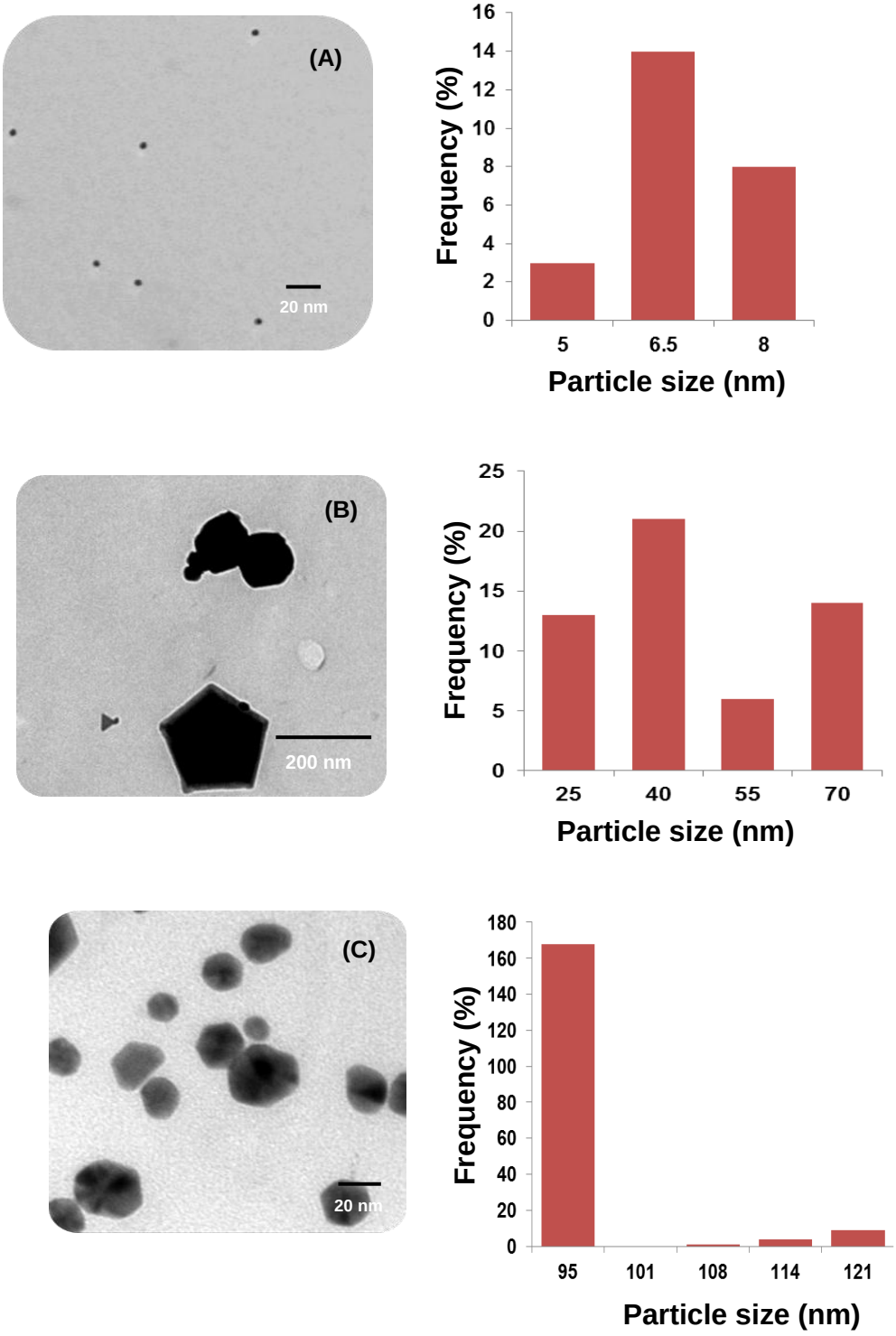

Fig. S31 Transmission electron microscope (TEM) images and size distribution of gold nanoparticles of (A) derivative **3** (B) derivative **4** (C) derivative **6**. Scale bar (A) 20 nm (B) 200 nm (C) 20 nm.

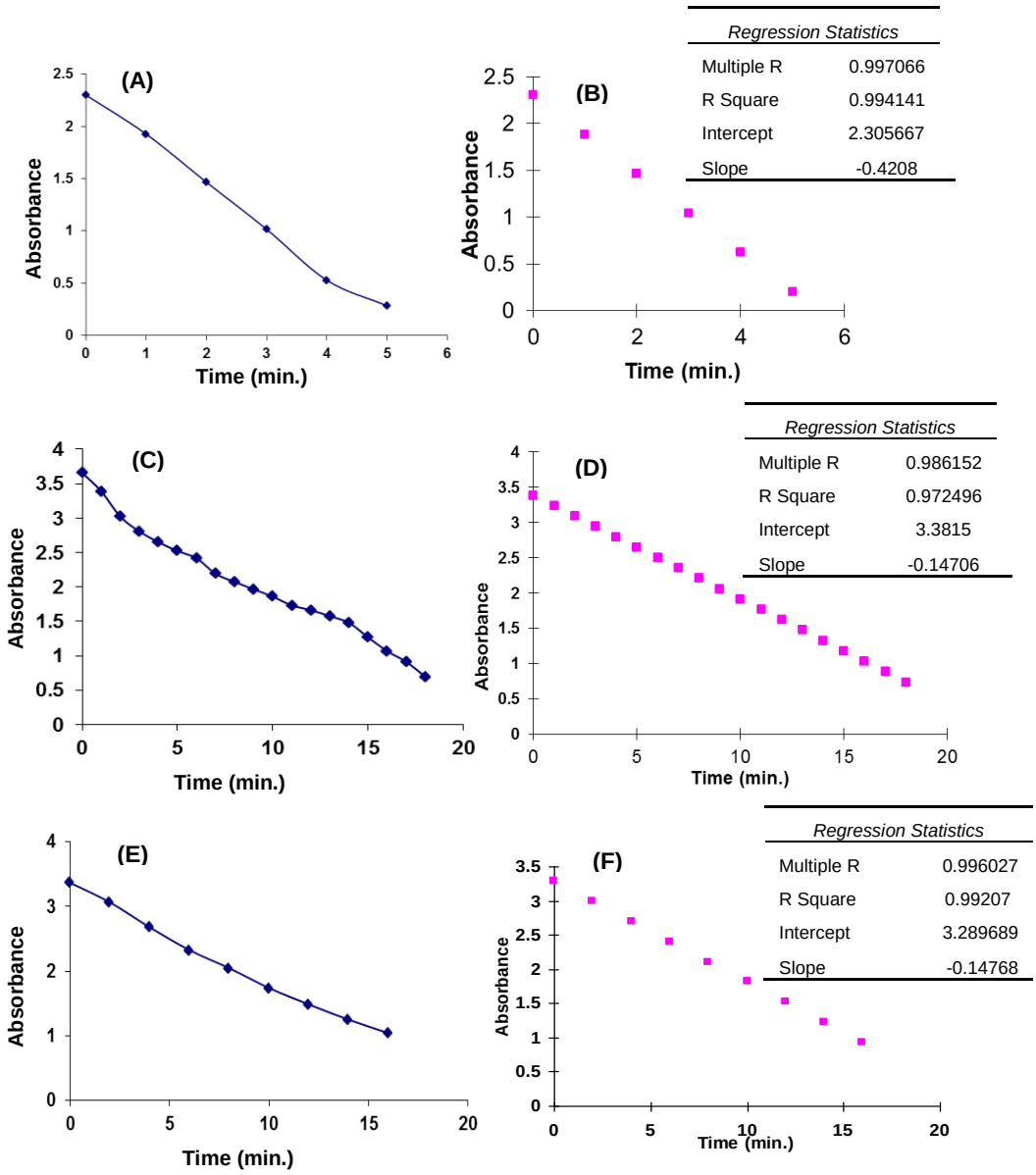

Fig. S32 Graphical representation of Time vs. absorbance plot and regression plot for the reduction of *p*-nitroaniline catalyzed by gold nanoparticles (A) and (B) of derivative **3** (C) and (D) of derivative **4** (E) and (F) of derivative **6**.

Catalytic reduction of *p*-nitroaniline follows Pseudo-first-order kinetics.[3] The apparent rate constants for the degradation of *p*-nitroaniline by gold nanoparticles of derivatives **3**, **4** and **6** listed in following table:

Gold nanoparticles	Rate constant
Derivative **3**	1.62×10^{-2} sec^{-1}
Derivative **4**	5.64×10^{-3} sec^{-1}
Derivative **6**	5.67×10^{-3} sec^{-1}

(3) Zelentsov, S. V.; Simdyanov, I. V.; Kuznetsov, M. V. *High Energy Chemistry* **2005**, *39*, 309-312.

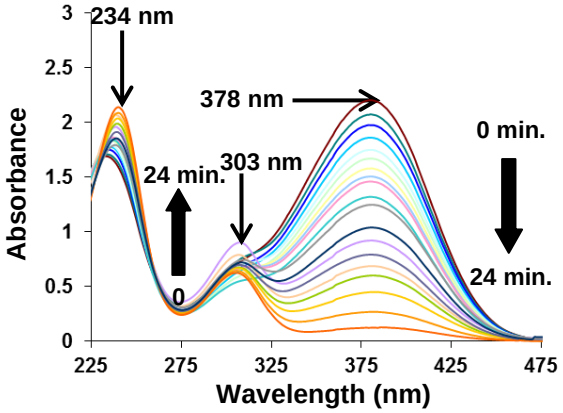

Fig. S33 UV-vis spectrum for the reduction of *p*-nitroaniline by adding $NaBH_4$ aqueous solution using gold nanoparticles of derivative **4** as catalysts.

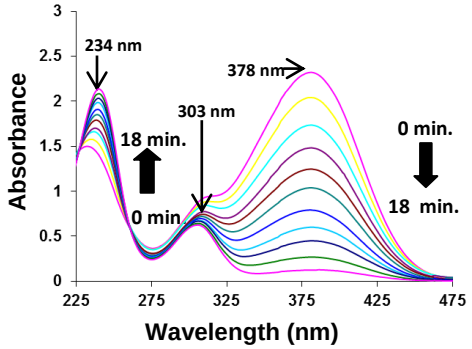

Fig. S34 UV-vis spectrum for the reduction of *p*-nitroaniline by adding $NaBH_4$ aqueous solution using gold nanoparticles of derivative **6** as catalysts.

^{1}H NMR of compound of *p*-phenylenediamine in $CDCl_3$

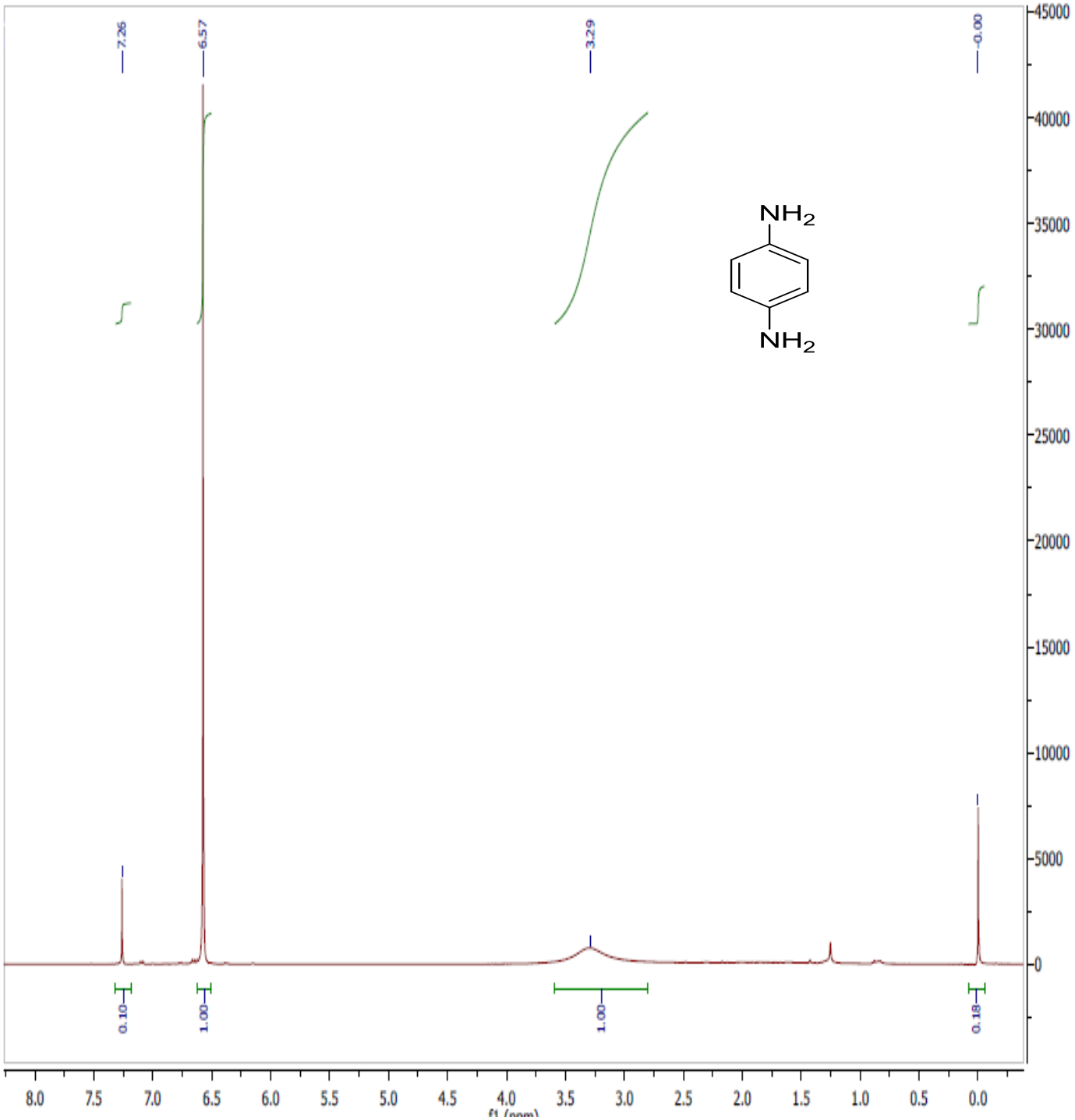

Fig. S35 ^{1}H NMR spectra of the reduced product *p*-Phenylenediamine in $CDCl_3$.

^{1}H NMR of compound **3** in $CDCl_3$

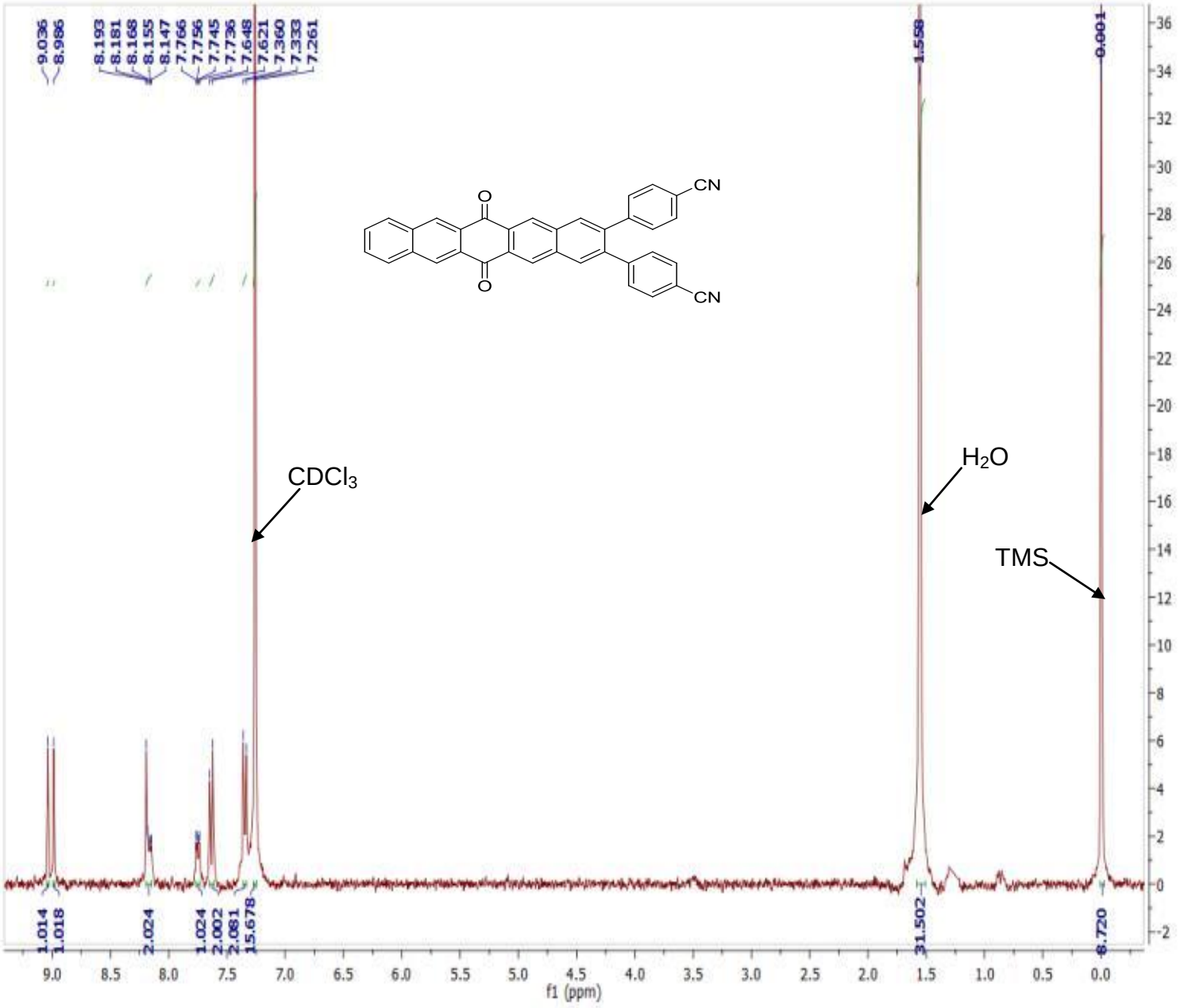

Fig. S36 ^{1}H NMR of spectrum of compound **3** in $CDCl_3$.

Mass spectrum of compound **3**

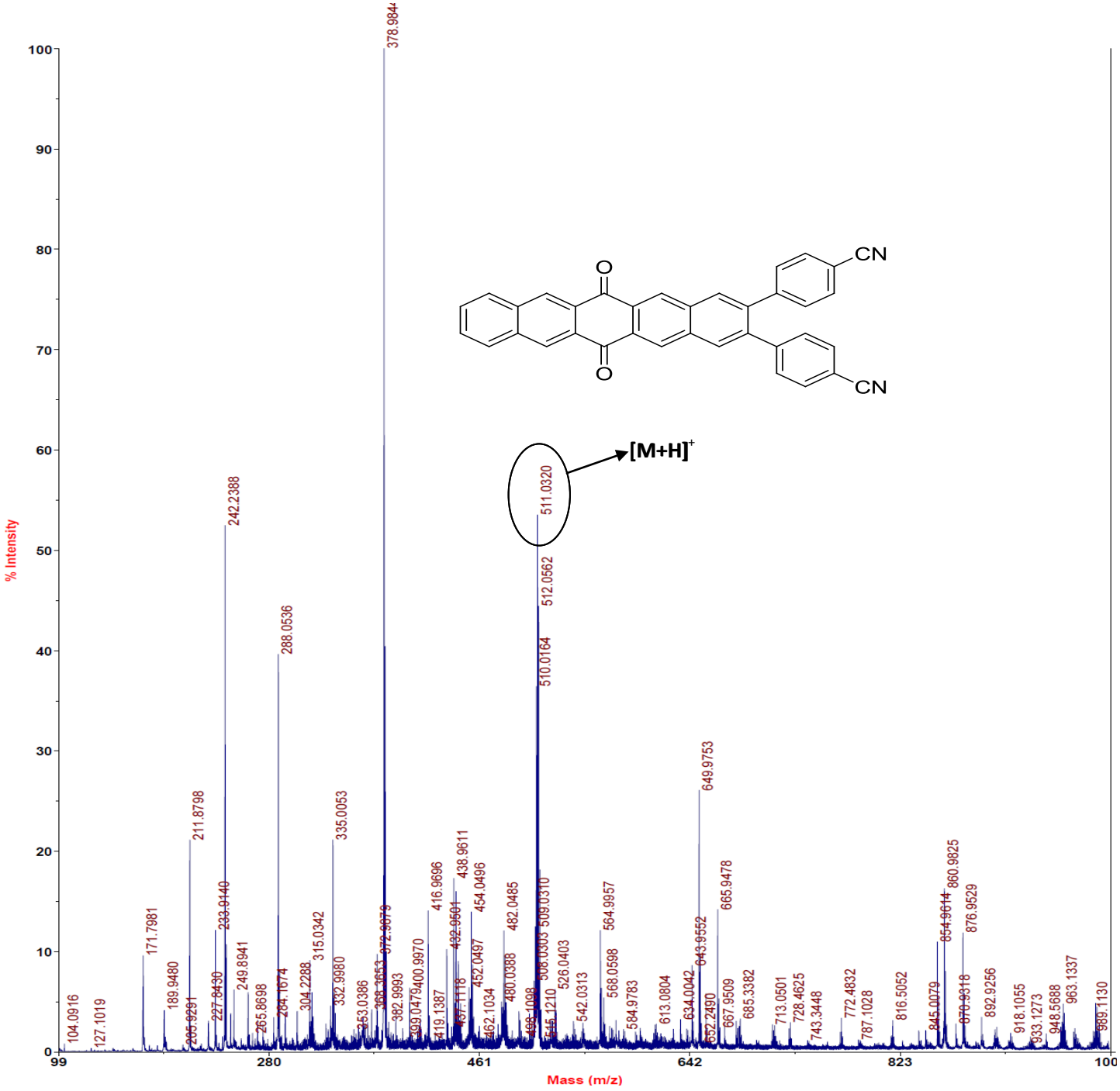

Fig. S37 Mass spectrum of compound **3.**

^{1}H NMR of compound **4** in $CDCl_3$

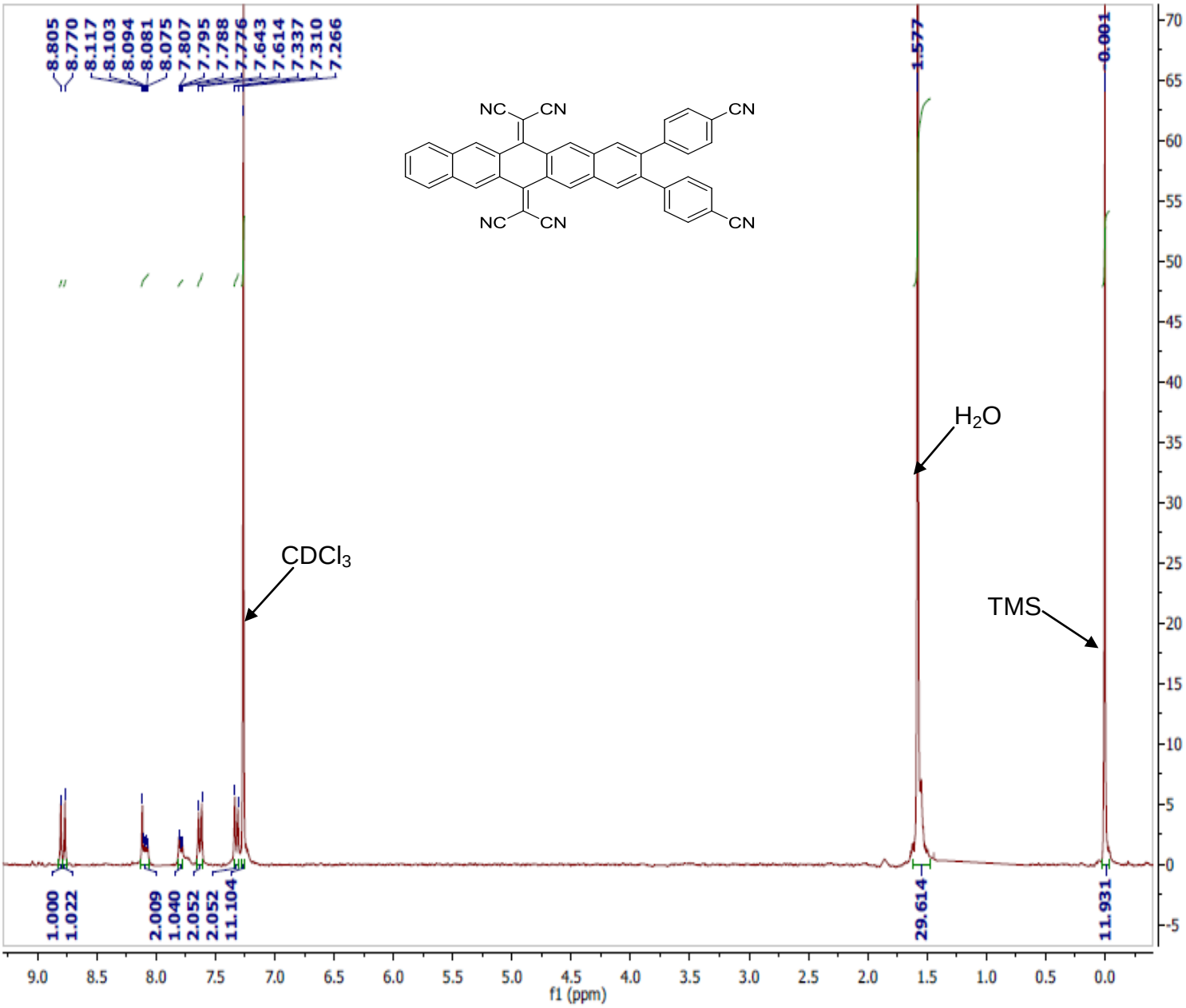

Fig. S38 ^{1}H NMR spectrum of compound **4** in $CDCl_3$**.**

^{13}C NMR of compound **4** in $CDCl_3$

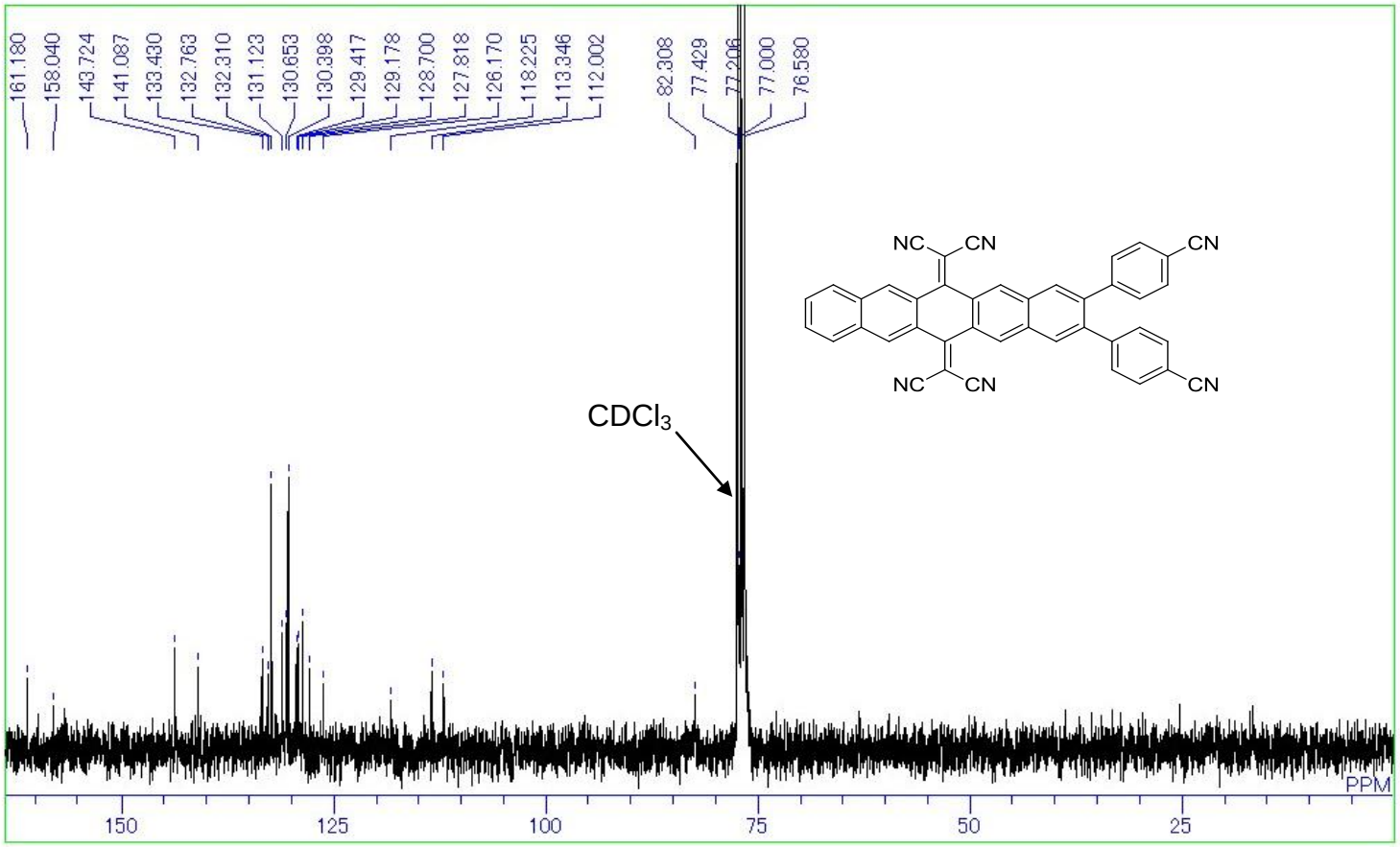

Fig. S39 ^{13}C NMR spectrum of compound **4** in $CDCl_3$**.**

Mass spectrum of compound **4**

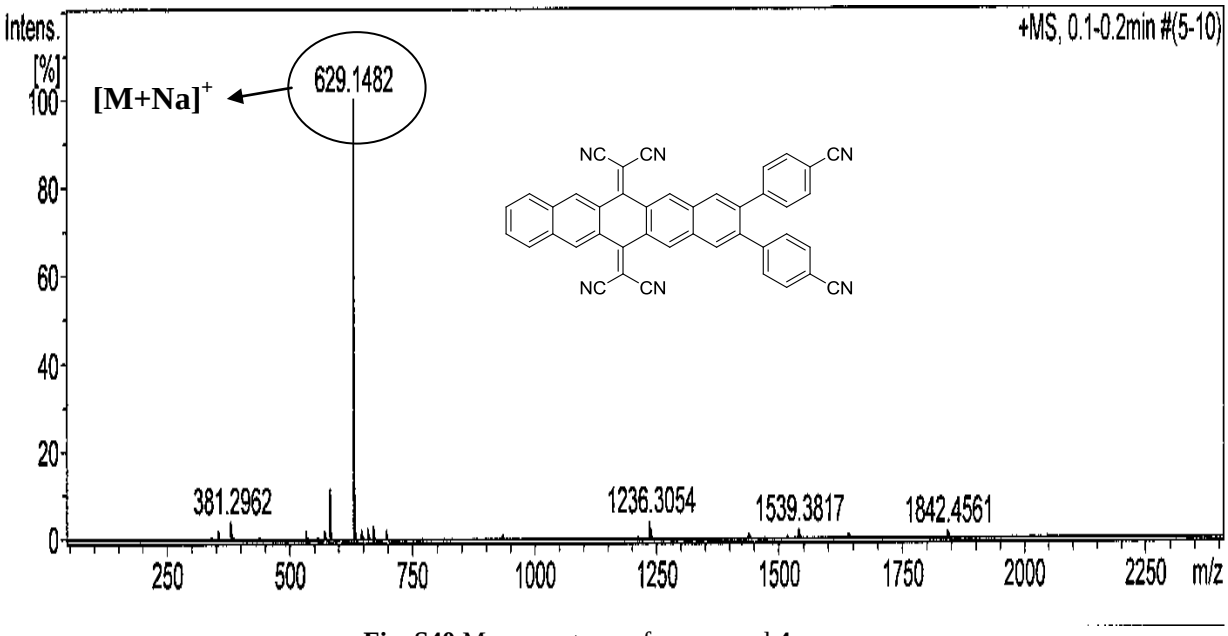

Fig. S40 Mass spectrum of compound **4.**

^{1}H NMR spectrum of compound **5**

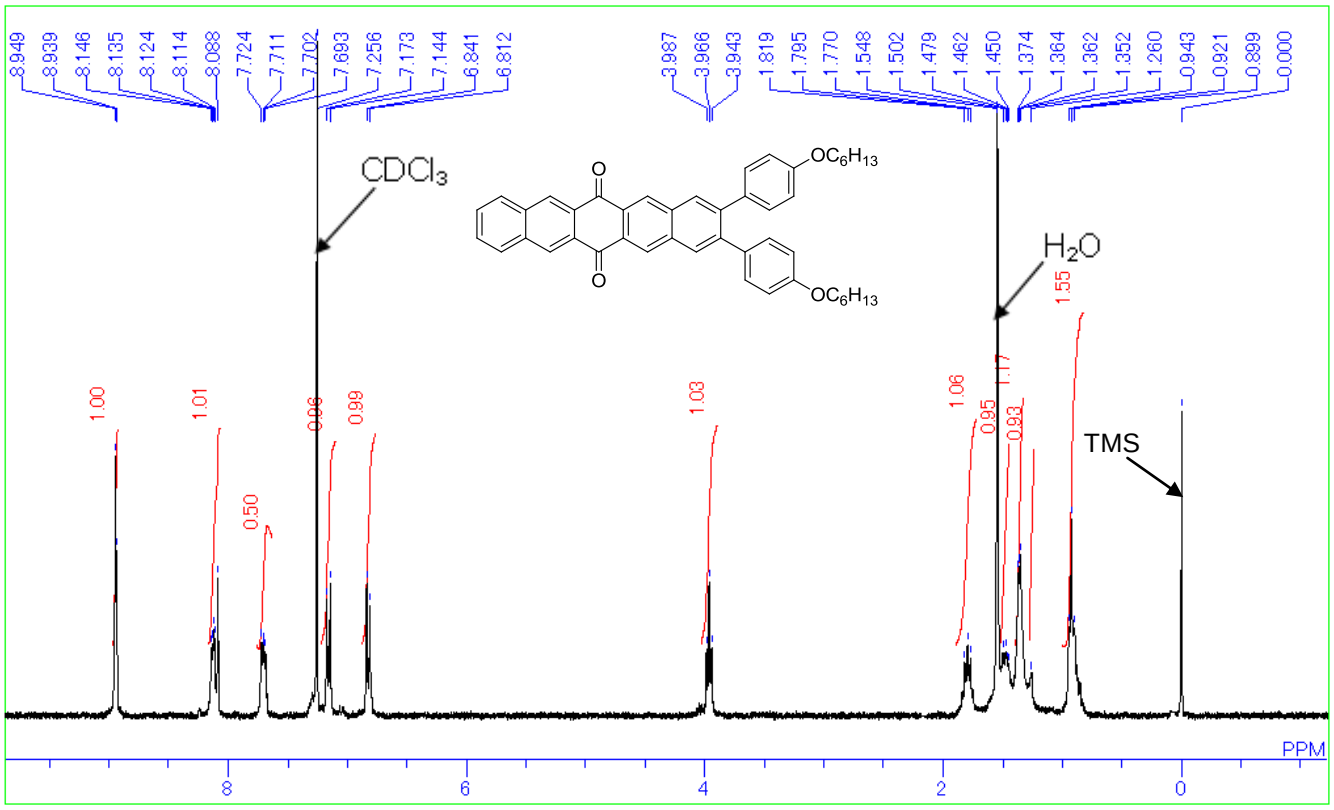

Fig. S41 ^{1}H NMR spectrum of compound **5** in $CDCl_3$

^{13}C NMR spectrum of compound **5**

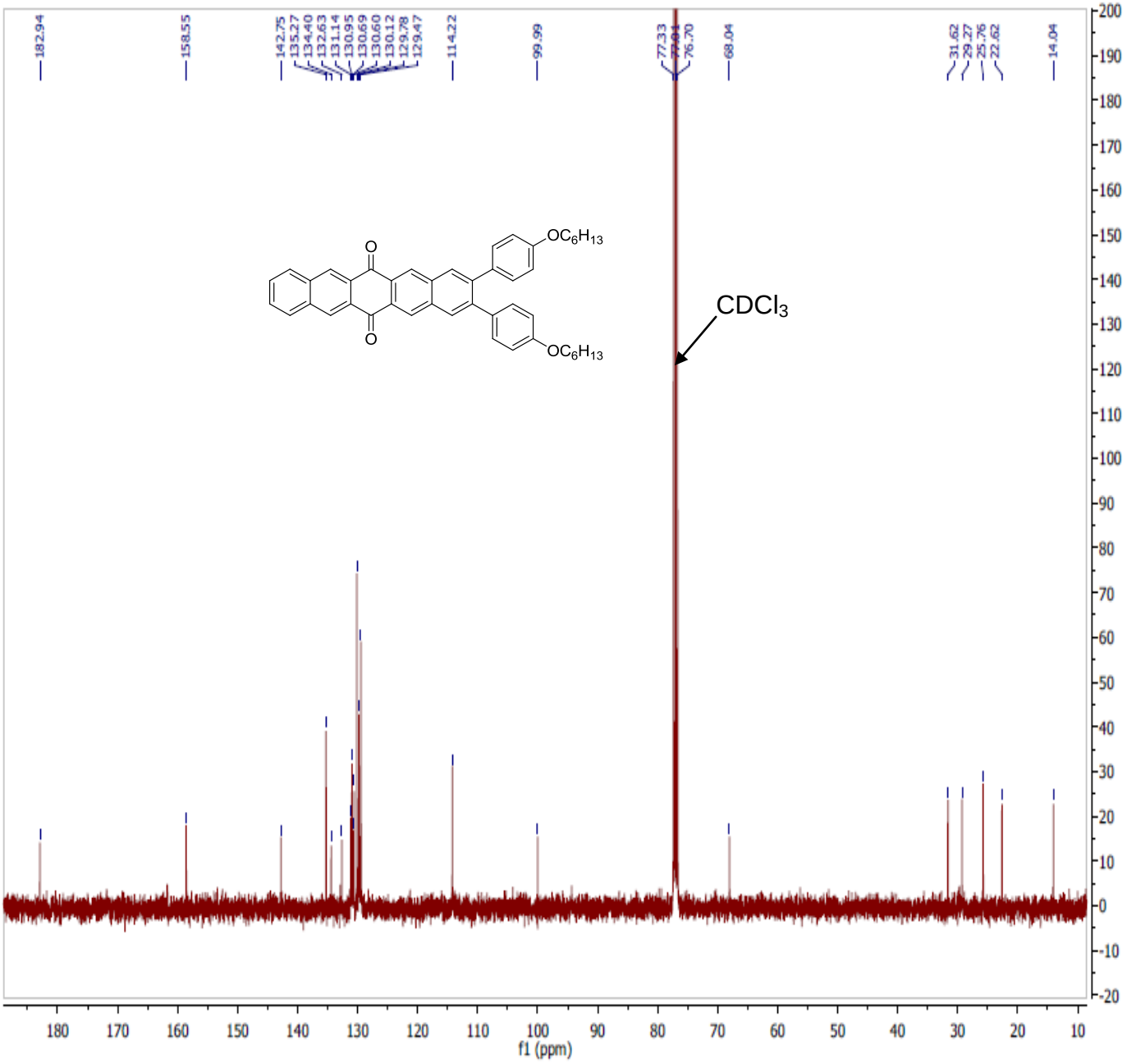

Fig S42 ^{13}C NMR spectrum of compound **5** in $CDCl_3$.

Mass spectrum of compound **5**

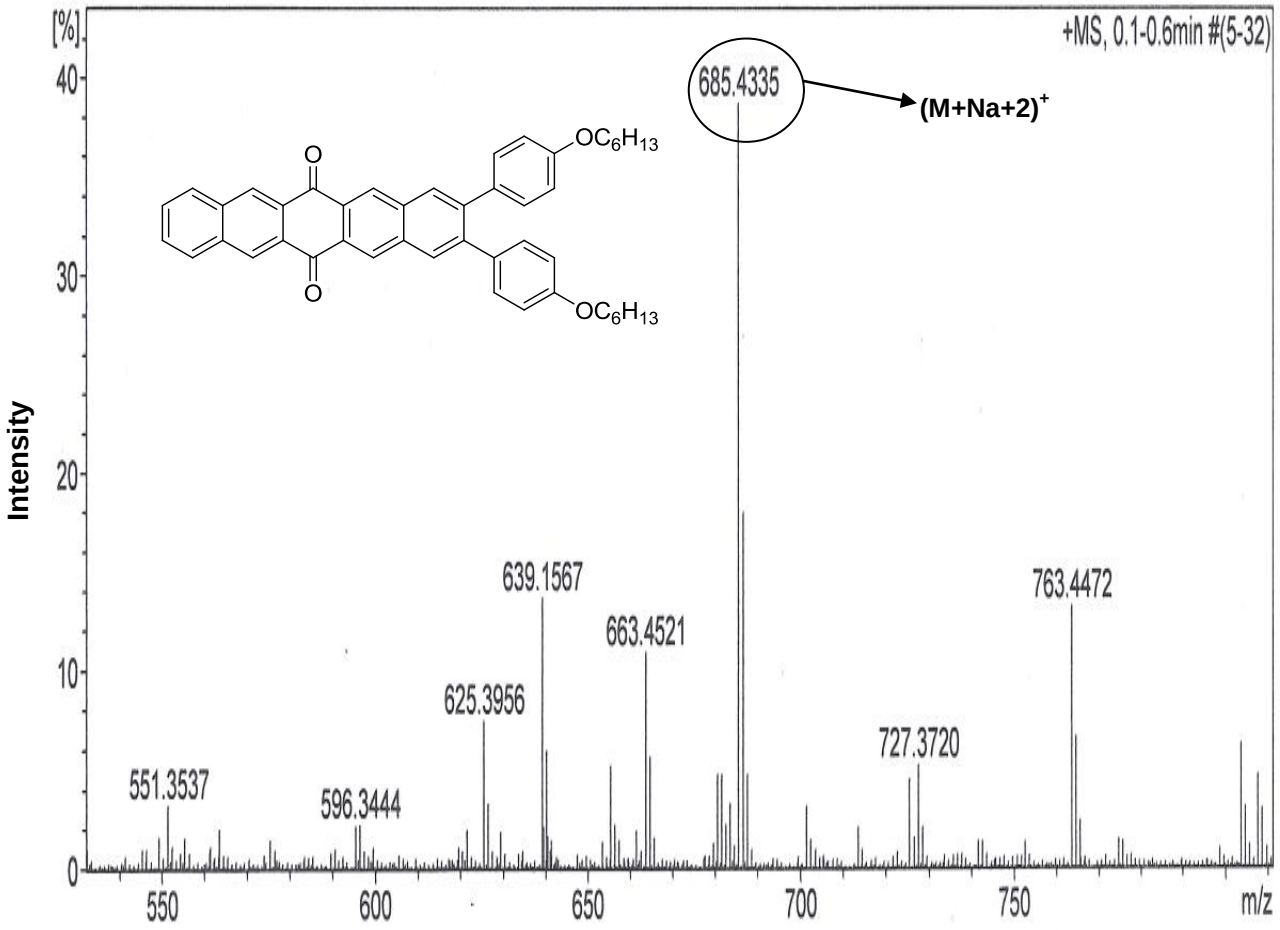

Fig. S43 Mass spectrum of compound **5**

^{1}H NMR spectrum of compound **6.**

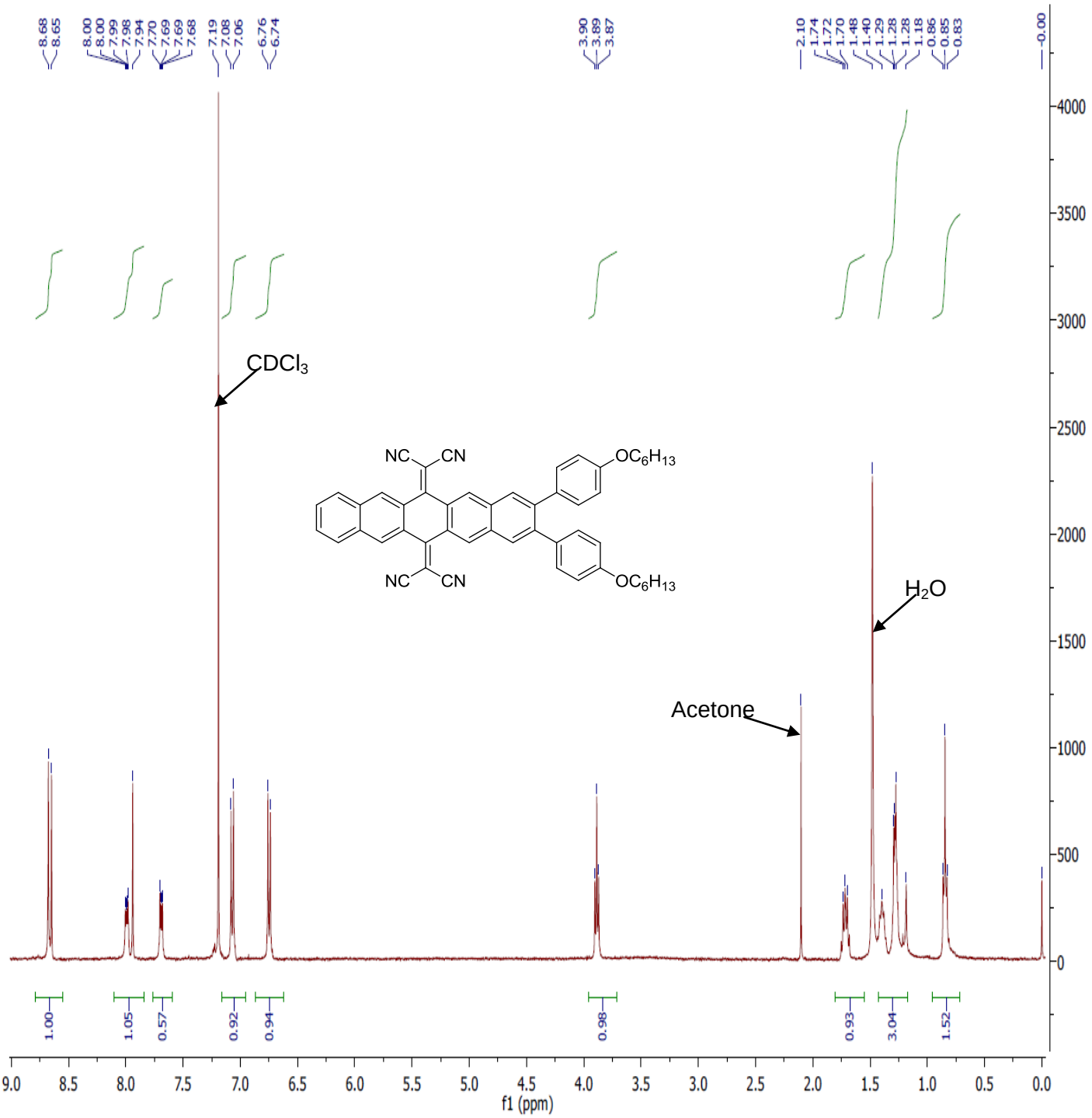

Fig. S44 ^{1}H NMR spectrum of compound **6.**

^{13}C NMR spectrum of compound **6**

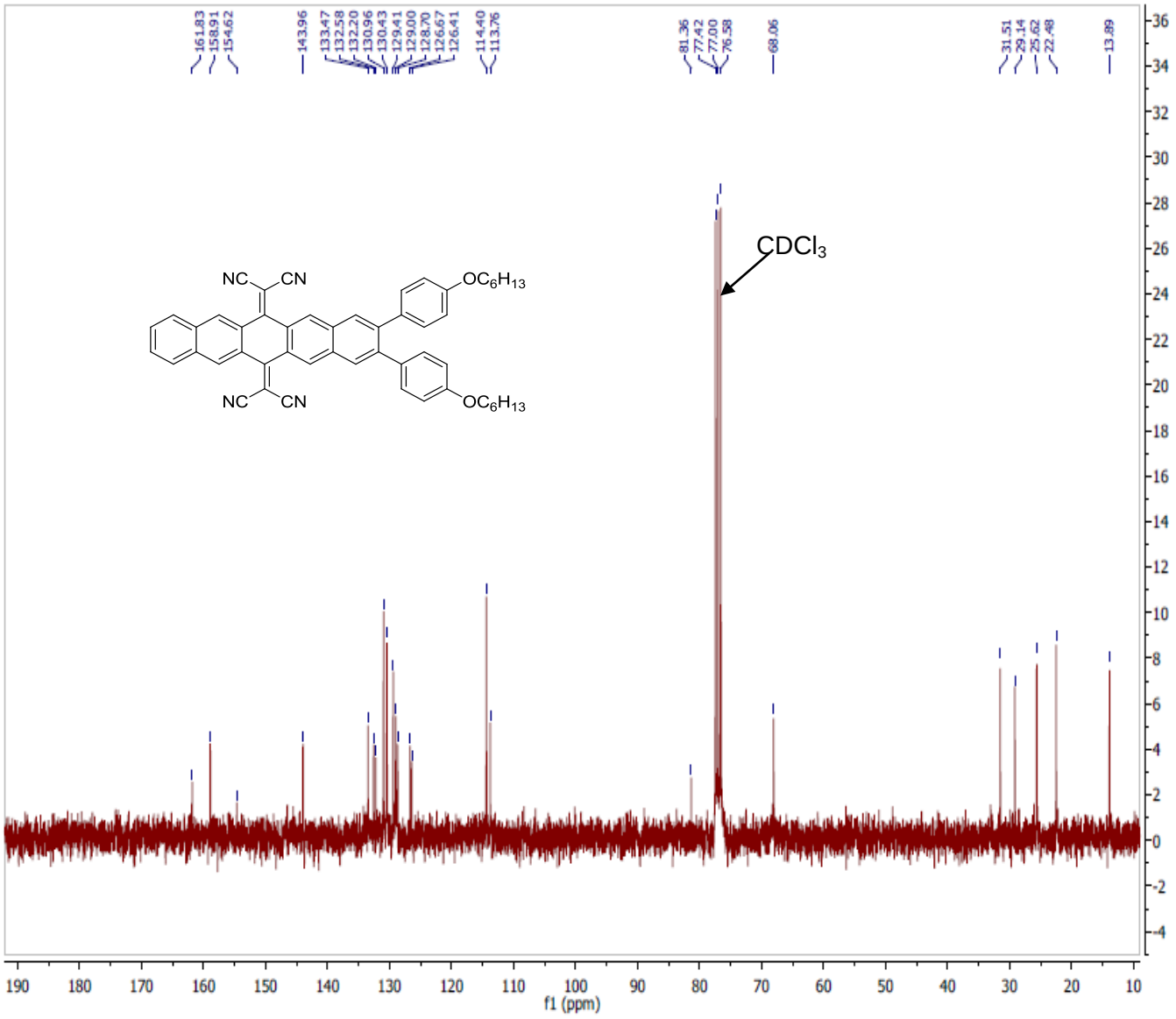

Fig. S45 ^{13}C NMR spectrum of compound **6.**

Mass spectrum of compound **6**

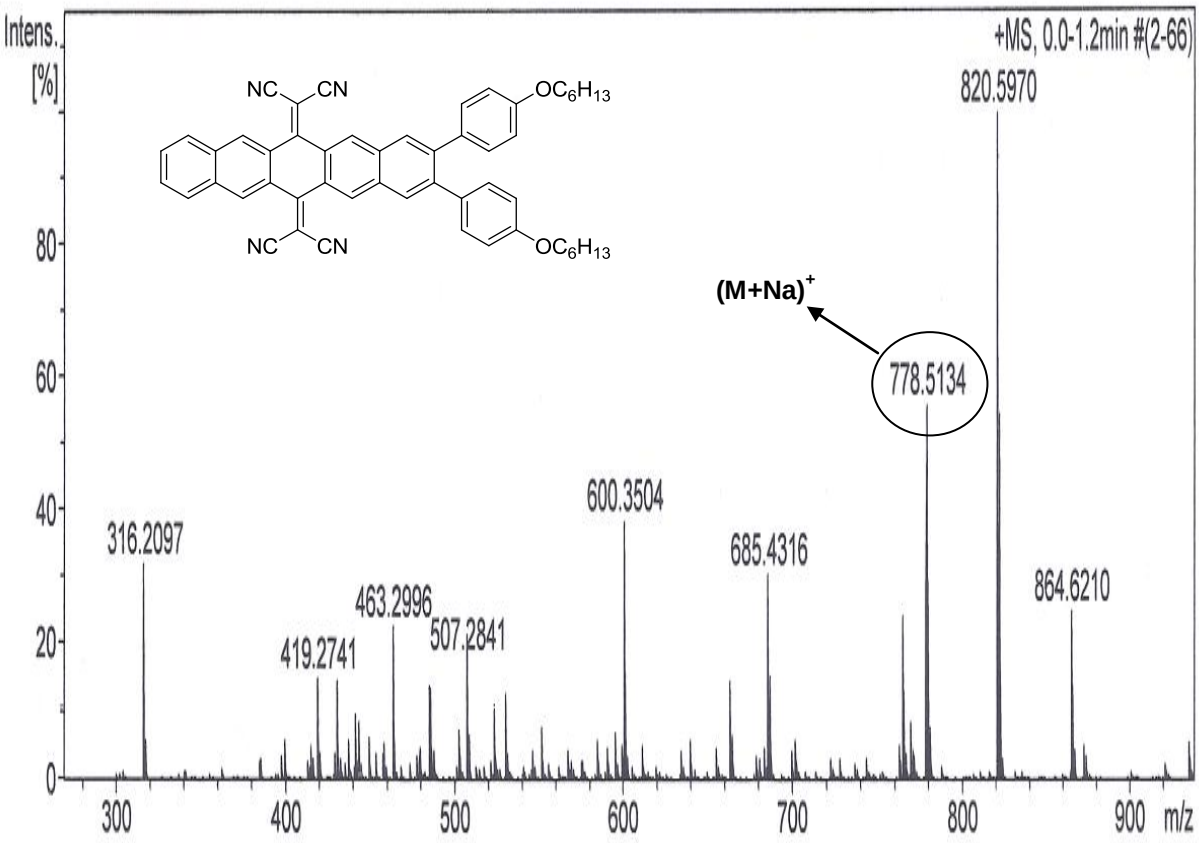

Fig. S46 Mass spectrum of compound **6**

Table S4: Comparison of relative efficiency of gold nanoparticles of derivative **3** over reported procedure in literature for the reduction of *p*-nitroaniline to *p*-phenylenediamine by iron metal.

Reaction time for the reduction of *p*-nitroaniline to *p*-phenylenediamine	catalyst	Journal
5 min.	Gold nanoparticles	Present manuscript
2.0 hours	Fe-Nano-ZSM-5	Ind. Eng. Chem. Res. **2013**, *52*, 11479
10.0 hours	Fe–phenanthroline/C	Chem. Commun., **2011**, *47*, 10972
3.0 hours	Iron(II) chloride tetrahydrate	Tetrahedron Lett. **2008**, *49* 1828
30 min.	Fe^{2+} ions	Journal of Hazardous Materials **2008**, *153*, 187